University of Cape Town

Department of Chemical Engineering

Improving the settleability of a metal sulphide suspension by the application of a magnetic field

Dissertation in fulfilment of the requirements for the degree of Master of Science in Engineering

PLAGIARISM DECLARATION

I know that plagiarism is wrong. Plagiarism is to use another's work and pretend that it is my own.

I have used the Harvard system for citation and referencing. In this report, all contributions to, and quotations from, the work(s) of other people have been cited and referenced.

This report is my own work. I have not allowed, and will not allow, anyone to copy my work

Signed Sibongiseni Gqebe_ Dated _23/07/2015_

Acknowledgements

I would like to thank my supervisor Prof Alison Lewis for her valuable input throughout the course of this work. Her guidance, wisdom and exceptional teaching skills have been an anchor throughout this journey. I am forever grateful for the opportunity she has given me. A special thank you must go to my co-supervisor, Dr Marcos Rodriguez-Pascual who not only masterminded but also helped me develop this project. His support, ideas and go-getting spirit have fuelled this work.

I would also like to thank Ms Hayley Battle and Dr Tracy Anne Craig for making CPU a delightful research group and for all the efforts they made in ensuring the success of my project.

To Jemitias Chivavava and Moses Nduna, thank you for always pushing me to challenge myself and for the time you both took to explain concepts that I battled to understand. You have been great sounding boards.

My sincere gratitude goes to all the CPU students for their valuable feedback, constructive criticism, professionalism and friendship. I am grateful to have shared this journey with such humble people.

To my mother Zukiswa Gqebe-Mwanda, thank you for being my biggest cheerleader, a constant light in my life and for being the inspirational woman you are. There is no greater love than a mothers love; you are testament to these words. A special thank you also goes to my brother and step father for their love and support.

Finally, I would like to thank the WRC and the John Davidson Trust for the financial support they provided.

Abstract

Gravitational sedimentation of suspensions in various precipitation processes is hindered by colloidal stability. More especially in sulphide precipitation, where high levels of supersaturation dominate and nucleation is favoured. This results in a large number of colloidal particles with a highly negative surface charge, which remain suspended in solution. The high surface charge of the suspension results in strong attraction/interaction between the ions on the particle surface and counter-ions in solution. Moreover, this strong interaction between ions on the particle surface and counter-ions in solution results in a charge build-up that renders the suspension stable. In order to induce gravitational sedimentation of these particles, a redistribution of ions close to the particle surface is required. This study therefore seeks to redistribute ions close to the particle surface by applying a magnetic field. This results in the reduction of inter-particle electrostatic repulsive forces and subsequent increase in the zeta potential of a suspension. For the purposes of this study, a copper sulphide suspension was used. A T-mixer was used as the reaction zone for the precipitation of each suspension. Subsequent to this, the suspended copper sulphide particles were exposed to a range of field strengths for set exposure times and their zeta potential was measured before and after exposure to the magnetic field. The effect of magnetic field strength, exposure time and particle speed on the zeta potential were tested. All particles had an initial zeta potential value equal to or less than - 40 mV prior to magnetic field exposure. A significant increase in zeta potential was observed with values reaching a maximum of - 16.5 mV when exposed to a 2 T field strength for 40 minutes. An increase in the zeta potential corresponds to a reduction in repulsive electrostatic forces between suspended particles due to the Lorentz force exerted by a magnetic field on the particle surface. DLVO plots were used to quantify this reduction in repulsive electrostatic forces.

Table of Contents

Table of Figures

List of Tables

Nomenclature

a activity [mol/dm^3]

a_i ion radius [m]

A_H Hamaker constant [J]

A area [m^2]

B magnetic field strength [T]

B_0 magnetic induction [T]

c concentration [mol/dm^3]

d distance between ion centres [m]

e elementary charge [C]

ε dielectric constant [C/V.m]

ε_0 electric permittivity of a vacuum

E electric field [V/m]

F Faradays constant [C]

F_E electric force [N]

F_L Lorentz force [N]

F_{vis} Liquid viscosity force [N]

H shortest distance between particle surfaces [m]

I ionic strength [mol/m3]

k^{-1} Debye-Huckel length [m]

k_d mass transfer coefficient [m/s]

k_r rate constant [1/s]

K_{sp} solubility product

λ_{12} London constant [-]

m mass [kg]

μ chemical potential [J/mol]

μ_E electrophoretic mobility [m^2 V s]

μ_0 magnetic permeability of a vacuum

η liquid viscosity [kg/ m s]

ρ charge density [C/m^3]

q electric charge [C]

r distance between particles [m]

R universal gas constant [J/mol.K]

S supersaturation

T temperature [K]

t time [s]

u particle velocity [m/s]

V_m magnetic dipole-dipole interaction [J]

V_R electrostatic repulsive potential [J]

V_T net interaction potential [J]

V_{vdW} attractive van der Waals potential [J]

ψ electrostatic potential [mV]

X magnetic susceptibility

Δx_i Lorentz ion shift [m]

z valence

ζ	zeta potential [mV]

1. Introduction

1.1 Background

Metal sulphide precipitation can be used as part of a hydrometallurgical process. Typically, it is used for treating industrial waste streams with high residual mixed metal ion concentration. Metal sulphide precipitation can also be applied in acid mine drainage treatment processes. Higher metal ion removal efficiencies over a broad pH range have been reported for sulphide precipitation when compared with the industrially prevalent hydroxide precipitation process (Feng et al, 2000). Moreover, in metal sulphide precipitation, sequential metal ion removal is possible due to the difference in the solubility products of various metal sulphides (Veeken et al, 2003). Sulphide precipitation does however have inherent drawbacks associated with it, such as the formation of fines. According to Lewis and van Hille (2006) in sulphide precipitation, fines form due to high levels of supersaturation caused by the extremely low solubilities of most metal sulphide salts. At these high supersaturation levels, the nucleation rate of crystals is favoured over the crystal growth rate (Lewis & van Hille, 2006; Mokone et al, 2010).

The formation of such fines hinders gravitational solid-liquid separation, which uses the force of gravity to separate a suspension into its individual components. This force of gravity is directly proportional to mass (Knight, 2008). In order to maximise separation efficiency, a large particle size is required. As a result, fine metal sulphides formed remain suspended in solution as they experience a small gravitational force and therefore exhibit slow settling rates.

Even though metal sulphide precipitation may achieve higher metal ion removal and the recovery of pure metal sulphide precipitates, the process is not widely used for the treatment of industrial waste streams. This is owing to the formation of large mixed precipitates, with reasonable settling rates, and low hydroxide reagent costs of the industrially prevalent hydroxide precipitation process. Fines formation and high sulphide reagent costs contribute to the infrequent use of metal sulphide precipitation in industry. Consequently, it is imperative to investigate techniques that limit the formation of fines

in metal sulphide precipitation or post precipitation techniques that may be used to improve the settling rates of metal sulphide fines.

Previous studies on metal sulphide precipitation focussed on reducing fines formation by controlling supersaturation. A study conducted by Mokone and co-workers (2010) showed that controlling the metal to sulphide molar ratio at a constant pH can improve the settling characteristics of metal sulphides. Work done by Nduna and collaborators (2013) showed that it is possible to alter the surface properties of copper sulphide particles and subsequently increase the settleability of these particles by varying the concentration of the dissolved lattice ions of a suspension and by partial oxidation. In both of these studies, the settling properties of metal sulphides were improved by either altering the chemical make-up of the system or further adding chemicals to the system. Although both studies achieved promising results, the addition of chemicals to achieve these results may exacerbate the environmental impact of the treated waste stream. As a result, it is necessary to investigate post precipitation techniques that enhance the settleability of metal sulphides without adding chemicals to a suspension.

1.2 Research Scope

Metal sulphide particles develop a highly negative surface charge in an aqueous suspension. This charge plays a significant role in the aggregation of particles as it determines the balance between the attractive van der Waals forces and the repulsive electrostatic forces between particles. A high surface charge indicates strong stability of particles in a suspension as a result of dominating electrostatic repulsive forces between them. The combination of high surface charge and fine particle size of metal sulphides leads to poor settling rates in gravitational solid-liquid separation.

This research therefore set out to study the settling rates of metal sulphide fines in order to improve their settling characteristics. This was done by altering the surface charge of copper sulphide particles in suspension using a magnetic field. For the purposes of this study, zeta potential was the measure used for colloidal stability. The zeta potential of all suspensions was measured before and after magnetic field exposure.

1.3 Plan of development

This dissertation is divided into seven chapters. The research background and scope are described in the introduction which is the first chapter. Chapter 2 comprises the theory section, which includes an overview of precipitation, particle rate processes, colloidal stability and electromagnetism. An extensive literature review on magnetic water treatment processes makes up chapter 3 followed by the methodology in chapter 4. This methodology section includes, chemical reagents used, an overview of the experimental setup, the experimental procedure and the analytical techniques used for both the precipitation and post precipitation steps. In Chapter 5 the results are presented and discussed. From these results conclusion are drawn and recommendations are made in chapter 6. A reference list follows in chapter 7.

2. Theory

2.1 Precipitation Overview

In general, precipitation refers to a rapid formation of a sparingly soluble solid phase from a liquid solution phase (Karpinski & Wey, 2002). According to Mullin (2001) and Karpinski and Wey (2002) precipitation is usually initiated at high supersaturation. Consequently, a chemical reaction is usually involved in precipitation, as the supersaturation required for initiating this process results from it.

The level of supersaturation in a precipitating solution governs the rates of component processes, such as nucleation and growth. The relation of the degree of nucleation to growth controls the product crystal size and size distribution crystallization processes (Myerson & Ginde, 2002). Due to the high levels of supersaturation in precipitation processes, nucleation is favoured (Mullin, 2001; Karpinski & Wey, 2002; Ulrich & Stelzer, 2011). This results in the formation of a large number of fine crystals.

Precipitation processes are of great importance as they are applied in various industries, such as pharmaceutical, paints and pigments and waste water treatment.

2.2 Supersaturation

Supersaturation is defined as the difference between the chemical potential of the solute in solution and the chemical potential of the solution in equilibrium with the solid phase. According to Myerson and Schwartz (2002) and Ulrich and Stelzer (2011) supersaturation is the fundamental driving force for crystallization and can be expressed as follows:

$$\frac{\mu - \mu^*}{RT} = \ln \frac{a}{a^*} \qquad 2.1$$

Where μ is the chemical potential, R is the universal gas constant, T is the absolute temperature, a is the activity and * denotes the property at saturation.

Mullin (2001) and Karpinski and Wey (2002) reported that for aqueous solutions of sparingly soluble electrolytes, supersaturation is best expressed in terms of the solubility product:

$$S = \frac{a_A a_B}{K_{sp}} \quad 2.2$$

Where *S* is supersaturation, *a* is the activity of the ionic species A and B and K_{sp} is the solubility product.

Generally, the activity cannot be easily determined. In such cases, supersaturation can be expressed as a concentration difference or as a ratio of concentrations:

$$\Delta c = c - c^* \quad 2.3$$

$$S = \frac{c}{c^*} \quad 2.4$$

Where *c* is the concentration and *c** is the saturation concentration.

2.3 Particle rate processes

2.3.1 Nucleation

The formation or birth of an ordered solid phase from a liquid or amorphous phase is known as nucleation (Ulrich & Stelzer, 2011). A build-up of supersaturation in a solid free solution results in nucleation (Karpinski & Wey, 2002). Nucleation may occur spontaneously or it may be induced by agitation, mechanical shock or extreme pressures within solutions or melts (Mullin, 2001).

There are two mechanisms by which nucleation may occur and they are primary and secondary nucleation. Primary nucleation is the formation of a solid phase in the absence of crystalline matter (Mullin, 2001). Secondary nucleation is the formation of a solid phase in the presence of crystalline matter. Figure 2.1 shows the mechanisms of nucleation:

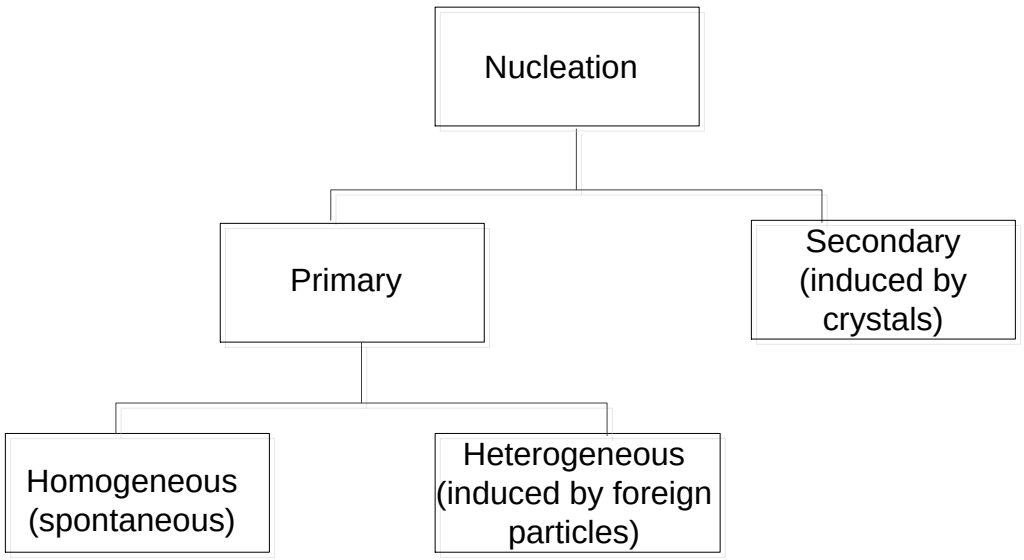

Figure 2.1: Mechanisms of nucleation (Mullin, 2001)

Primary nucleation can be categorized as either homogeneous or heterogeneous. Homogeneous primary nucleation is the formation of a solid phase without the presence of foreign particles. While heterogeneous primary nucleation is the formation of a solid phase that is induced by the presence of foreign solid particles.

2.3.2 Growth

According to Myerson and Ginde (2002), the growth of a crystal can be measured in two ways: (1) as the change in some dimension of the crystal with time and (2) as the change in mass of a crystal with time. The first description is referred to as the linear growth rate and has dimensions of length per unit time.

Immediately after stable nuclei have formed in a supersaturated system, they begin to grow into crystals of visible size (Mullin, 2001; Karpinski & Wey, 2002). This occurs through a sequence of the following two steps: the mass transport of the growth units from the supersaturated bulk solution to the crystal-solution interface by bulk diffusion and the integration of these growth units to the crystal lattice by surface reaction processes. The slower of the two steps controls the overall rate of crystal growth (Karpinski & Wey, 2002).

Figure 2.2 is a depiction of the crystal-solution interface of the two step crystal growth mechanism:

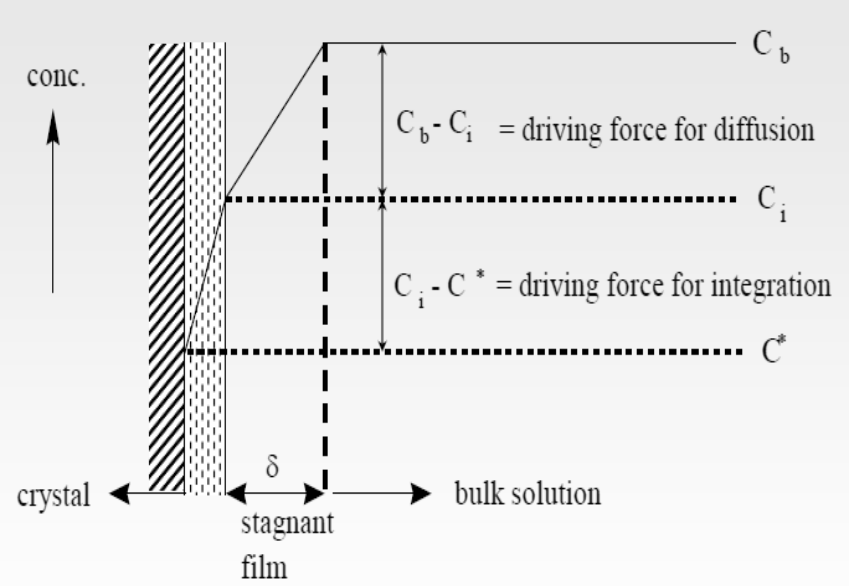

Figure 2.2: Crystal-solution interface (Mullin, 2001)

Mullin (2001) states that these two steps occur under the influence of different concentration driving forces and can be represented by the following equations:

$$\frac{dm}{dt} = k_d A\,(c - c_i) \qquad 2.5$$

$$\frac{dm}{dt} = k_r\,A\,(c - c^*) \qquad 2.6$$

Where m is the mass of solid deposited in time t, k_d is the coefficient of mass transfer by diffusion, k_r is the rate constant for the surface reaction, A is the surface area of the crystal, c is the solute concentration, c_i is the solute concentration in the solution at the crystal-solution interface and c^* is the equilibrium concentration.

2.3.3 Aggregation

Aggregation is a size enlargement process, which involves the collision and subsequent adhesion of particles to form a new larger particle (Bramley, 1997). The particles in an

aggregate cluster are held together by weak attractive van der Waals forces. Hartel and co-workers (1986) suggested that aggregation consists of two mechanistic steps: The collision of particles by Brownian motion, laminar shear flow or turbulent flow and the staying together of particles, which is controlled by forces due to surface potential.

The aggregation of particles may be described quantitatively by the theory of Derjaguin, Landau, Verwey and Overbeek also commonly referred to as the DLVO theory (Overbeek et al, 1977).

2.3.4 Agglomeration

Agglomeration is also a size enlargement process, which involves the collision and adhesion of particles to form a new large particle. The distinction between aggregation and agglomeration are the mechanisms that drive each process. In agglomeration, particles are cemented together by the formation of crystal bridges between them. Hartel and co-workers (1986) defined an agglomerate as a tightly bound mass formed by the cementation of individual particles by chemical forces. Hounslow and collaborators (1988) reported that the agglomeration rate is directly proportional to supersaturation. Consequently, agglomeration can only be achieved in the presence of supersaturation.

2.4 Mixing

The crystallization kinetics of soluble substances is influenced by hydrodynamic conditions (Karpinski & Wey, 2002). Consequently, the mixing of reagents plays a crucial role in precipitation processes, as this affects the degree and distribution of suspersaturation and ultimately crystal characteristics such as size and morphology.

2.4.1 Fluid flow characterization

Fluid flow is typically characterised into two regimes: laminar and turbulent (Weigl et al, 2003; Capretto et al, 2011). The distinction between these two regimes is the relative

importance of viscous to inertial forces, which is measured by the Reynolds number (Green, 2002).

A low *Re* indicates laminar flow. Green (2002) states that in this flow system, viscous forces dominate, fluid streams flow parallel to each other and convective mass transport occurs only in the direction of fluid flow. At high *Re*, inertial forces dominate as turbulent flow is observed. In this flow system, fluid streams exhibit random motion in space and time and convective mass transport occurs in all directions. As a result, turbulent flow results in better dispersion of fluid and enhanced mixing quality (Capretto et al, 2011).

According to Green (2002), the nature of turbulence in a vessel has a great effect on the mixing and the crystallization process itself. Turbulent fluctuations are associated with eddies of various length scales. In an agitated tank, turbulence is generated by an impeller. This impeller creates large scale eddies, which in turn create smaller eddies. This proceeds until a limit, which is commonly referred to as the Kolmogorov length scale, is reached (Deen, 1998) (as cited by Green, 2002).

2.4.2 Macromixing

Macromixing carries fluid (by convection) from the feed points to the rest of the vessel. It is associated with large length scales created by an impeller. These length scales are roughly equivalent to the vessel dimensions (Green, 2002; Karpinski & Wey, 2002). In the absence of macromixing, the concentration of reagents within a vessel would build up around the feed location and not be blended with the rest of the vessel. Consequently, macromixing is essential for vessels

2.4.3 Mesomixing

Mesomixing is described as the turbulent diffusion of the feed with the surrounding fluid (Green, 2002; Karpinski & Wey, 2002). It is associated with length scales length scales that are equivalent to the diameter of the feed pipe. According to Green (2002) in the

immediate vicinity of the feed point, mixing of the concentrated feed into the fluid is achieved by mesomixing and then micromixing. As a result, the length scales created by mesomixing form an environment for micromixing (Green, 2002; Karpinski & Wey, 2002).

2.4.4 Micromixing

Micromixing is the intimate mixing at molecular length scales. These molecular length scales dominate below the Kolmogorov scale (Green, 2002). Micromixing takes place by unsteady molecular diffusion within energy dissipation vortices (Karpinski & Wey, 2002). Consequently, it provides more contact surface area between reagents. This generates a uniform distribution of supersaturation and results in a narrow particle size distribution.

Micromixing is the fastest turbulent mixing sequence at the smallest length scale. According to Karpinski and Wey (2002) it is of crucial importance in precipitation because the rate at which particle rate processes occur is very fast. Therefore, fast mixing of reagents is required. Moreover, chemical reaction, nucleation and crystal growth are molecular level processes and only mixing on the molecular scale can directly influence their course (Baldyga & Bourne, 1984).

2.5 Particle surface charge

When an electrolyte solution is in contact with another phase, such as a solid, gas or another liquid immiscible with the electrolyte, a spontaneous redistribution of ions between the two phases takes place (Overbeek, 1984; Derjaguin et al, 1987). It follows that surfaces acquire a surface electric charge when brought into contact with a polar medium such as water. This may be due to one of the following mechanisms:

1. Surface ionisation - charge may be acquired through the dissociation of surface groups, such as carboxyl and amino groups.

2. Ion adsorption - excess concentrations of positive or negative ions influence the adsorption of ions on a surface. The nature of ions adsorbed on a surface determines the surface charge.
3. Ion dissolution - charge may be acquired by the unequal dissolution of the oppositely charged ion of which the particles are composed.

2.6 Colloidal stability

According to Overbeek (1982) colloids are defined as dispersed systems of a particle size, between 1 nm and 1 μm, where sedimentation by gravity plays a minor role. This is because colloids are so small in size that inter-particle forces are much more important than the pull of gravity (Overbeek, 1982). Colloidal stability is sometimes defined as the tendency to resist aggregation due to inter-particle repulsion caused by an electric charge on the particles, an electrical double layer of sufficient strength or chemically bound large molecules/ steric stabilization (Ottewill, 1977; Overbeek, 1982). The potential difference between the particle surface and the bulk liquid is known as the zeta potential, which is involved in most electrokinetic flows (Velev and Bhatt, 2006). The zeta potential magnitude can be related to particle stability, a high magnitude of zeta potential indicates strong particle stability.

In colloidal dispersions, particles come into contact with each other due to Brownian motion. However, this contact does not result in permanent contact or binding between particles.

2.7 van der Waals Forces

van der Waals forces are attractive between two approaching colloidal particles of the same nature (Overbeek, 1977; Hartel, 1986). It follows that loss of colloidal stability and subsequent attraction between particles, in the absence of electrostatic repulsion, are due to attractive van der Waals forces. Ottewill (1977) and Overbeek (1984) reported that the van der Waals energy, V, between two molecules is inversely proportional to the sixth

power of the distance between them. This energy may be quantified via the following equation (Overbeek, 1984):

$$V = -\frac{\lambda_{12}}{r^6} \qquad 2.7$$

Where λ_{12} is the London constant and r is the distance between the particles.

2.8 Electrical double layer

Collectively, the particle surface, Stern layer and diffuse layer make up the electrical double layer (Derjaguin et al, 1987). In the fluid layer closest to the particle surface, there is strong adsorption of counter-ions. This is commonly known as the Stern layer. Co-ions are repelled by the particle surface. However, they exist in the diffuse layer where both co-ions and counter-ions are found as mobile ions that are adsorbed in equilibrium with one another. Figure 2.3 illustrates the structure of the electrical double layer.

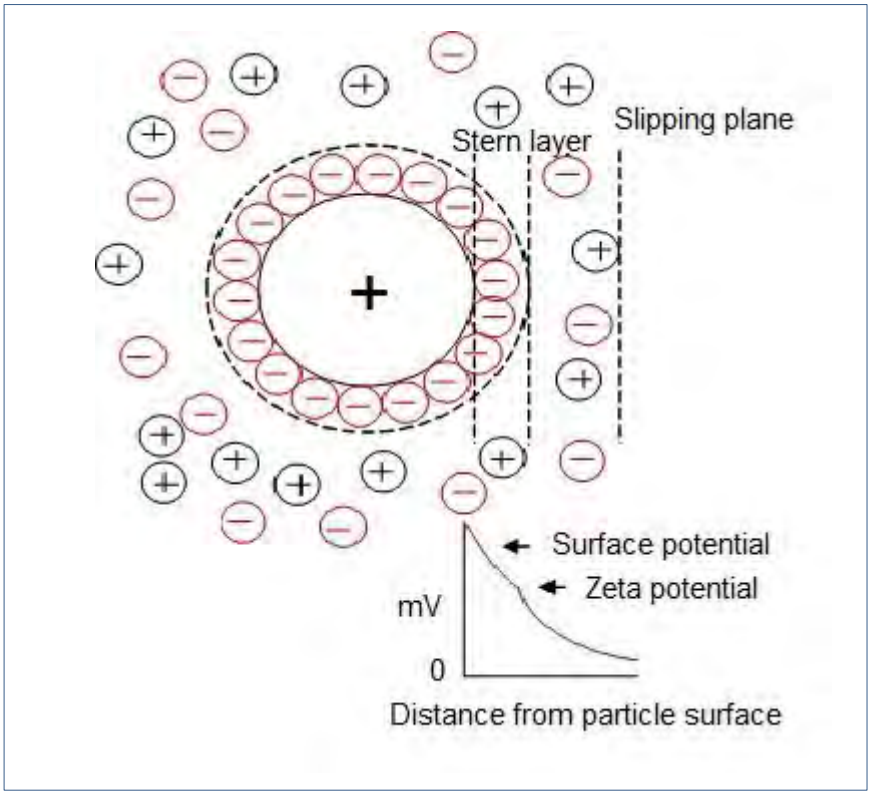

Figure 2.3: Structure of the electrical double layer of a surface in an aqueous medium adapted from (Schneider, 2011)

In a colloidal dispersion, each particle possesses this electrical double layer. The double layers of neighbouring particles interact with one another as a result of electrostatic and osmotic forces between the ions and the surfaces (Overbeek, 1977; Derjaguin et al 1987). Ottewill (1977) and Overbeek (1977) reported that when particles approach one another, the interaction of their double layers results in repulsion between them if they are of the same chemical nature and have surface charges and surface potentials of the same sign and magnitude. This repulsion is due to the ions adsorbed on the particle surfaces.

The basic structure of the electrical double layer can be described by the theory proposed by Gouy (1910) and Chapman (1913) (as cited by Derjaguin et al 1987; Overbeek, 1984). According to this theory, the particle charge is considered as a spread out surface charge on a plane. The counter charge is carried by the counter-ions in the Stern layer.

This theory excluded the diffuse layer as part of the electrical double layer (Derjaguin et al, 1987).

Boltzmann revised the theory of Gouy (1910) and Chapman (1913) to include the diffuse layer. According to Boltzmann, the counter charge is carried by all the ions in solution. The ionic distribution of the electrical double is described by the Boltzmann equation as follows:

$$c_+(x) = c_0 \exp\left(-\frac{z^+ e\psi(x)}{kT}\right) \qquad 2.8$$

$$c_-(x) = c_0 \exp\left(\frac{z^- e\psi(x)}{kT}\right) \qquad 2.9$$

Where c_+ (x) is the concentration of positive ions at a distance x from the charged surface, c_- (x) is the concentration of the negative ions at a distance x from the charged surface, c_0 is the concentration of ions where ψ is zero, z^+ is the valance of the positive ions, z^- is the valance of the negative ions, *e* is the elementary charge, kT is the thermal energy and ψ is the electrostatic potential at a distance x from the charged surface.

By equations 2.7 and 2.8, if the surface charge of a particle at some distance x is positive, there will be a surplus of negative ions surrounding that particle. By equations 2.7 and 2.9, the converse is true.

Although the Gouy-Chapman theory may be used to describe the structure of the electrical double layer, at high potentials unrealistic counter-ion concentrations are approximated near a particle surface (Chan et al, 1976; Overbeek, 1982). A solution to this problem was provided by Stern (1924) (as cited by Overbeek, 1982). Stern suggested that counter-ions cannot approach a particle surface closer than a distance δ, which corresponds to the radius of the counter-ions. Figure 2.4 illustrates the idea proposed by Stern (1924).

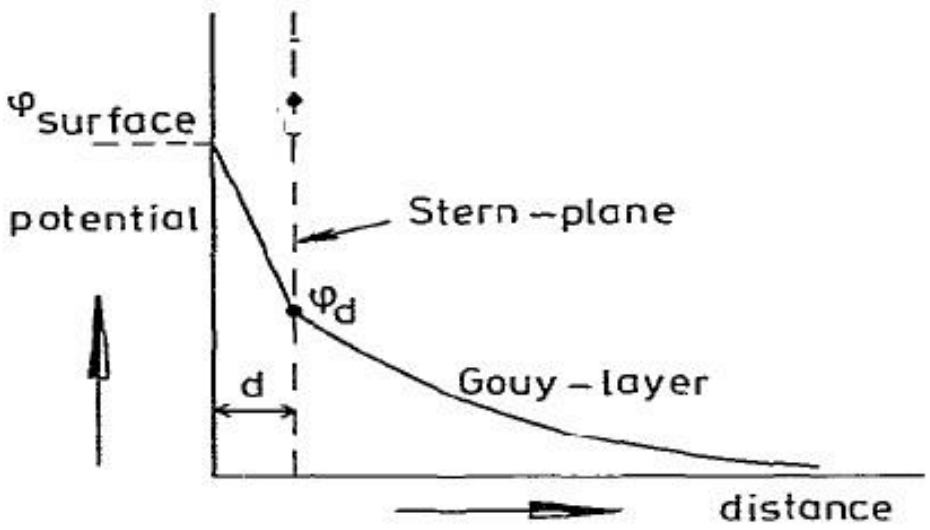

Figure 2.4: Stern-Gouy model of the electrical double layer (Overbeek, 1982)

According to Chan et al (1976) and Overbeek (1984) charge density and the electrostatic potential can be related using the following Poisson equation:

$$\frac{d^2\psi\,(x)}{dx^2} = \frac{\rho\,(x)}{\varepsilon\varepsilon_0} \qquad 2.10$$

Where ρ (x) is the charge density at some distance x, ε is the dielectric constant of the medium and ε_0 is the permittivity of a vacuum.

The Poisson-Boltzmaan equation (2.11) grew from equations 2.8 and 2.9 via the following relation (Chan et al, 1976; Overbeek, 1984):

$$\rho\,(x) = \; c_+(x)z_+ \; + c_-(x)z_- \qquad 2.11$$

$$\frac{d^2\psi\,(x)}{dx^2} = \frac{2zec_0}{\varepsilon} sinh\frac{ze\psi}{kT} \qquad 2.12$$

When equation 2.11 is linearized the solution becomes:

$$\psi\,(x) = \; \psi_0 \exp(-kx) \qquad 2.13$$

From equation 2.13 one may deduce that at constant charge density, the electrostatic potential of the double layer decreases as an exponential function of distance (Chan et al, 1976; Overbeek, 1984).

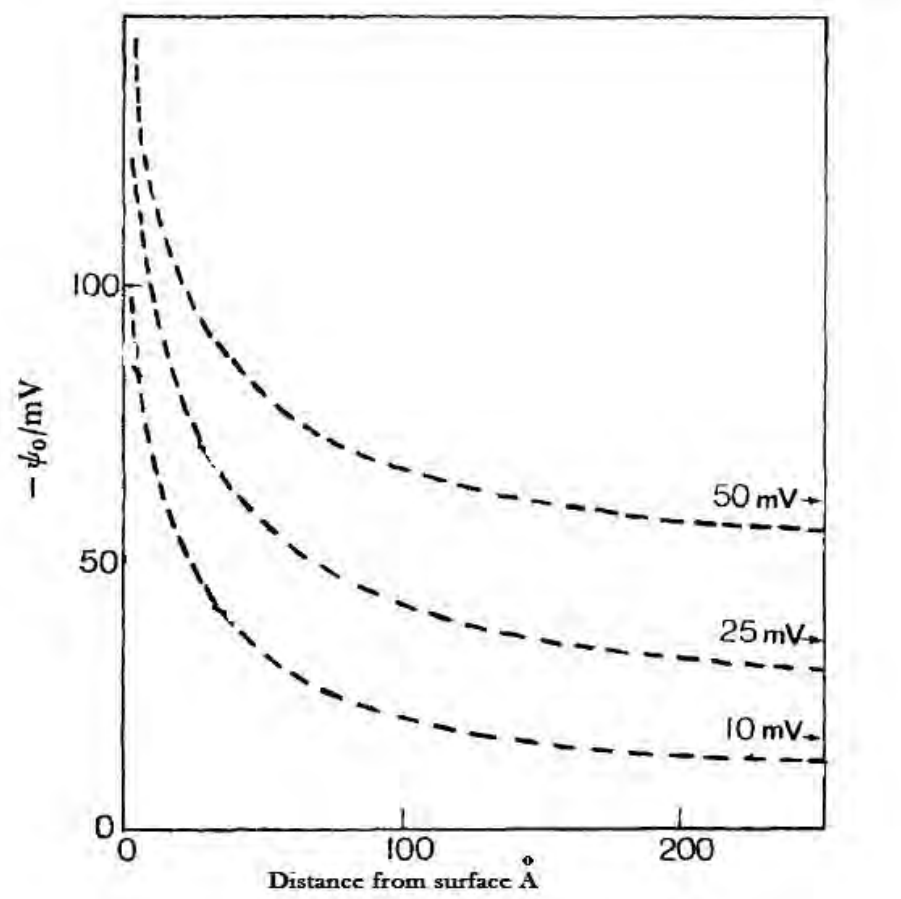

Figure 2.5: Exponential decay of electrostatic potential with distance at constant charge density (Chan et al, 1976)

Figure 2.5 depicts graphically the relationship between electrostatic potential and distance from the particle surface at a constant charge density.

According to Derjaguin and co-workers (1987) and Overbeek (1984), the thickness of the electrical double layer is commonly referred to as the Debye-Huckel length and is quantitatively described by equation 2.14:

$$\frac{1}{k} = \sqrt{\frac{\varepsilon\varepsilon_0 RT}{2F^2 I}} \qquad 2.14$$

Where R is the universal gas constant, F is Faradays constant, k^{-1} is the inverse Debye length and I is the ionic strength of the medium.

The ionic concentration therefore strongly affects the electrical double layer. This is because by equation 2.14, the Debye length, which is a characteristic of the electrical double layer thickness, is inversely proportional to the square root of the ionic concentration of a solution. At high ionic strengths, colloids aggregate due to the screening of the charge on the colloids by the electrical double layer (Ottewill, 1977; Overbeek, 1977; Hartel et al, 1986). The converse is also true: at low ionic strengths the colloids remain dispersed. This makes the ionic strength a key parameter in determining the interaction energy between particles as the electrical double layer is the sole contributor to the electrostatic repulsive force between particles. As a result, the balance between the van der Waals attractive force and the electrical double layer repulsive force determines the stability of colloidal dispersions (Attard, 2001; Chan, 2006; Ohshima, 1995).

2.9 DLVO theory

The theory of Derjaguin and Landau (1941) Verwey and Overbeek (1948) quantitatively approximates the rate of coagulation of colloidal suspensions (Dejaguin et al, 1987; Karpinski & Way, 2002). According to this theory, there is an energy barrier that must be surmounted before two particles can come into contact. The magnitude of this energy barrier is determined by the interplay of the attractive van der Waals forces and the repulsive electrostatic forces between suspended particles (Ottewill, 1977; Overbeek, 1977; Derjaguin et al, 1987; Kaprinski & Way, 2002). This energy barrier may be quantified by the following equations (Overbeek, 1977):

$$V_T = V_R + V_{vdW} \qquad 2.15$$

Where V_T is the net interaction energy, V_R is the electrostatic repulsive force and V_{vdW} is the attractive van der Waals force.

$$V_{vdW} = -\frac{A_H}{6}\left[\frac{2a_i^2}{d^2-4a_i^2} + \frac{2a_i^2}{d^2} + \ln\frac{d^2-4a_i^2}{d^2}\right] \qquad 2.16$$

Where A_H is the Hamaker constant, a_i is the ion radius and d is the distance between the centres.

$$V_R = 2\pi\varepsilon\varepsilon_0 a\psi^2 exp^{-kH} \qquad 2.17$$

Where H is the shortest distance between particle surfaces.

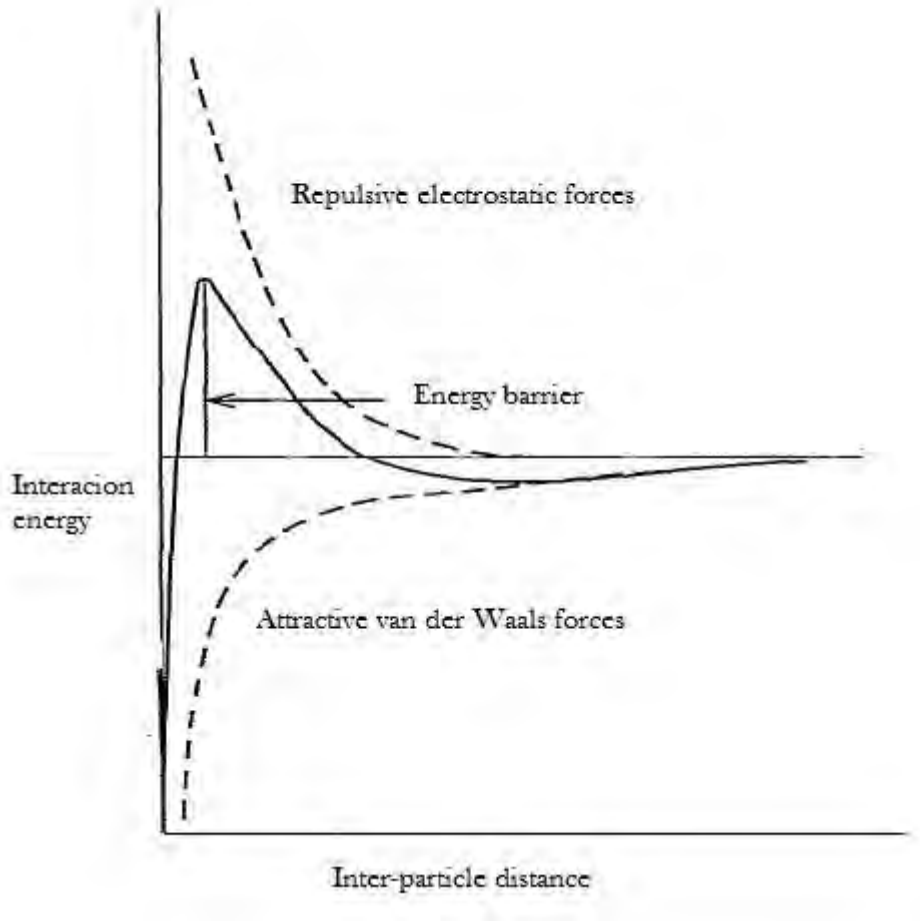

Figure 2.6: Energy barrier between suspended particles (Overbeek, 1982)

Figure 2.6 illustrates the interplay between attractive and repulsive forces. When repulsive electrostatic forces dominate, the overall interaction energy lies in the positive region and the energy barrier reaches an absolute maximum. When attractive van der Waals forces dominate, the overall interaction energy lies in the negative region and the energy barrier is eliminated.

2.10 Electrophoresis

Electrophoresis is the motion of charged suspended particles as a result of a uniform electric field (Weigl et al, 2003). This is in agreement with the force per charge ratio of a

particle which shows that electric force is proportional to charge and electric field via the following equation:

$$F_E = qE \tag{2.18}$$

Where F_E is the electric force, q is the particle charge and E is the electric field. The major electrophoretic characteristic of a particle is the electrophoretic mobility, μ_E, which is defined as follows:

$$\mu_E = \frac{u}{E} \tag{2.19}$$

Where u is the particle velocity and E is the electric field. From equation 2.19, it may be deduced that the electrophoretic mobility, is the ratio of the velocity of a particle in an electric field to the strength of that field (Weigl et al, 2003). Electrophoretic mobility is related to zeta potential via the following equation (Velev & Bhatt, 2006):

$$\mu_E = \frac{2\varepsilon\varepsilon o\zeta}{3\eta} \tag{2.20}$$

Where ε and ε_o are the dielectric permittivity of the media and vacuum respectively, ζ is the zeta potential and η is the liquid viscosity. According to equation 2.20, increasing the zeta potential of a particle increases the electrophoretic mobility while a decrease in mobility is observed with an increase in medium viscosity.

The mechanism behind electrophoresis may be explained by the following two steps: an electric field is applied to particles suspended in an electrolyte; this field exerts a force on the particles that induces migration of these charged particles towards oppositely charged electrodes (Bebie et al, 1998; Weigl et al, 2003; Velev & Bhatt, 2006). This technique is mostly used to separate molecules, pull together colloidal particles and to transport nano and micro fluidic devices.

2.11 Electromagnetism

A magnetic field can be generated in one of two ways: by permanent magnets or it can be induced by an electric current (Knight, 2008). The latter is commonly referred to as an electromagnetic field. It must be noted that a magnetic field is only created by moving

electric charges. As stated by Knight (2008), a magnetic field is created at all points in space surrounding a current carrying wire. A magnetic field is visually illustrated by magnetic field lines. These lines form loops with no beginning or ending point. This shows that a magnetic field is continuous through a region of space. This is illustrated on Figure 2.7.

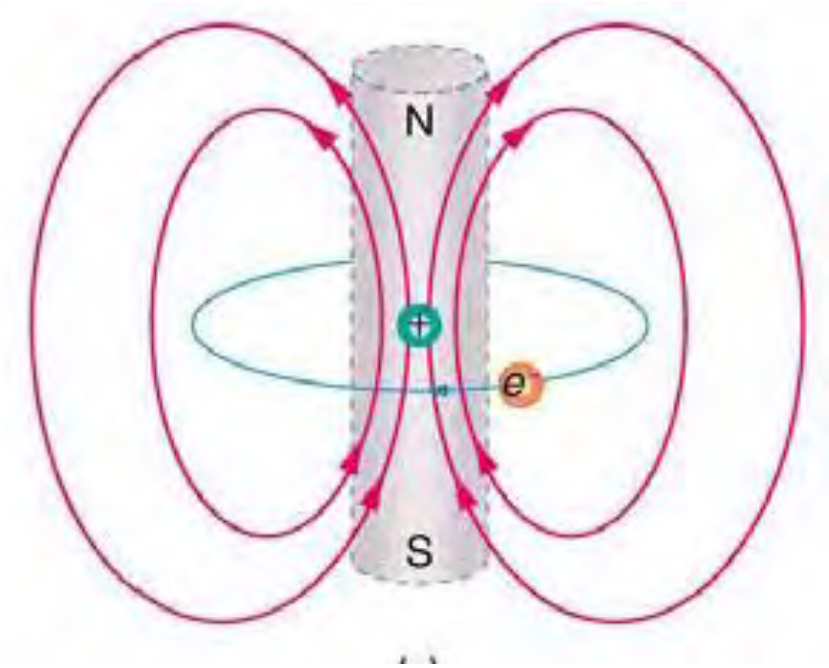

Figure 2.7: An electron orbits a nucleus forming a closed current loop which produces a magnetic field with a north and south pole (Knight, 2008)

The magnetic field at each point has both magnitude, which is referred to as the magnetic field strength, and direction. It follows that magnetic field strength is a vector quantity.

2.11.1 Lorentz force

When a charged object moves through a magnetic field, a force is exerted onto the object (Knight,2008; Zaidi et al, 2013). This force is known as the Lorentz force and may be quantified using the following equation:

$$F_L = quB \qquad 2.21$$

Where F_L is the Lorentz force, q is the charge and B is the magnetic field strength.

2.11.2 Magnetic properties of transition metal ions

An electron has a magnetic dipole moment due to its quantum mechanical spin (Silberberg, 2006). As a result, an electron generates a small magnetic field as though it is a spinning charge. When an orbital is filled with two electrons with opposite spin numbers, two opposing fields are created, one that is attracted to an external magnetic field and one that is repelled by an external magnetic field. These result in a net dipole moment that is equal to zero as the opposing fields created cancel one another (Silberberg, 2006). When an orbital is filled with one electron, a single field is created that is attracted to an external magnetic field. This results in a net magnetic dipole moment.

According to Silberberg (2006) a species with unpaired electrons in an orbital exhibits ferromagnetism. Ferromagnetic metal ions have a positive magnetic susceptibility and are attracted to a magnetic field. In contrast a species with no unpaired electrons exhibits diamagnetism. Diamagnetic species have a negative magnetic susceptibility and are repelled by magnetic fields.

3. Literature review

3.1 Metal sulphide precipitation

The application of metal sulphide precipitation for the treatment of heavy metal rich wastewater streams is practised in industry. Although this process is not commonly practiced, it has been reported to achieve lower residual metal effluent concentrations than the widely used hydroxide precipitation (Feng et al, 2000; Veeken et al, 2003). Metal sulphide precipitation is inherently driven by high levels of supersaturation (van Hille & Lewis, 2006; Mokone et al, 2010). As a result, colloidal metal sulphide precipitates are formed, which make solid-liquid separation by gravitational sedimentation increasingly difficult due to their small particle size. Commonly, flocculants are used to improve the sedimentation of colloids, thus adding further impurities to waste water streams. Consequently, supersaturation control is crucial in metal sulphide precipitation.

3.1.1 Supersaturation

According to van Hille and Lewis (2006) and Mokone and collaborators (2010), high supersaturation levels in metal sulphide precipitation are due to the extremely low solubilities of most metal sulphide salts. By definition solubility is the ability of a solute to be dissolved in a solvent (Mullin, 2001). The extent of this dissolution is known as the saturation concentration. Kirwan and Orella (2002) stated that the solubility of amphoteric compounds is strongly dependent on pH because the predominant form existing in solution changes with the hydrogen concentration. Metal ions such as copper, zinc and lead form amphoteric compounds in aqueous solutions. It follows that the solubilities of these metal compounds are a function of pH. The solubility of various metal sulphides as a function of pH was thermodynamically modelled by Lewis (2010) and is presented in Figure 3.1.

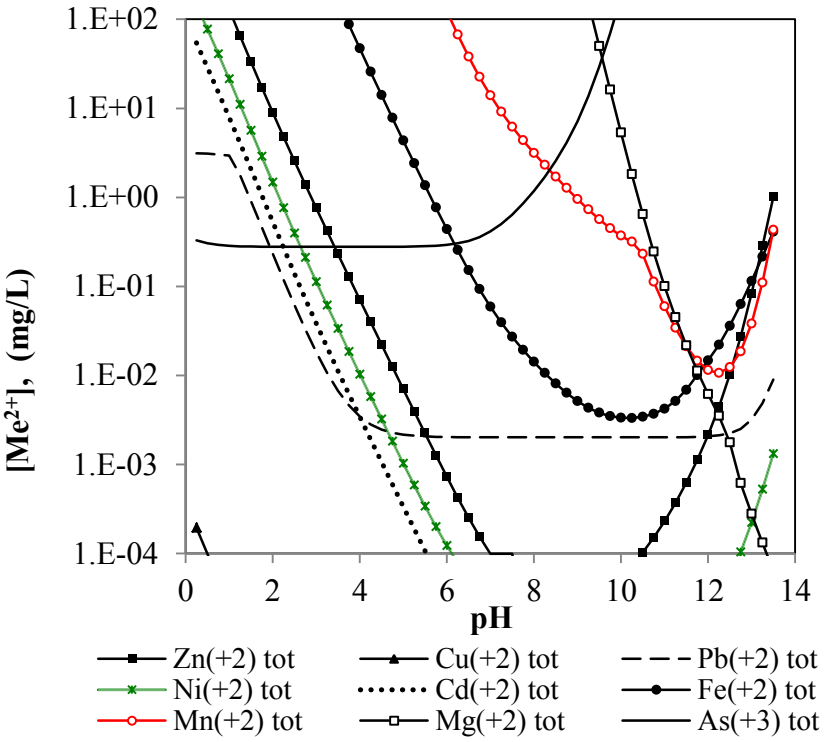

Figure 3.1: pH dependence of metal sulphide solubilities (Lewis, 2010)

From Figure 3.1 one may deduce that the pH may be used as a means to control the level of supersaturation in sulphide precipitation.

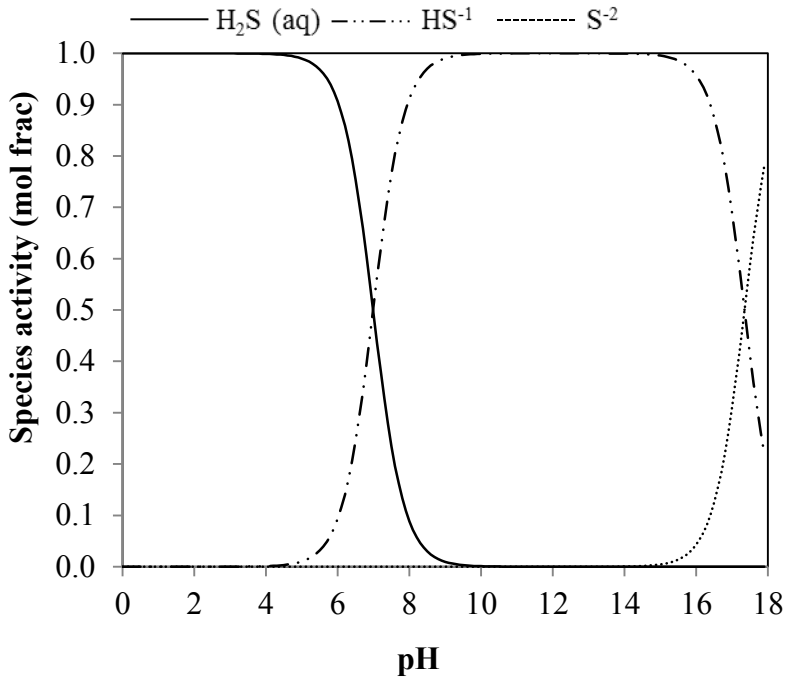

Figure 3.2: pH dependence of sulphide speciation (Lewis et al, 2010)

The speciation of aqueous hydrogen sulphide at various pH values is shown in Figure 3.2. The following may be deduced from this plot: At pH values less than 6, the concentration of H_2S (aq) in the bulk solution will be high, alkaline solutions with $8 \leq$ pH < 16 will be rich in HS^- ions and at pH value > 16 the concentration of S^{2-} ions in the bulk solution will be high. This is in accordance with findings by Jackson (1986) which suggested that the aqueous speciation of sulphide and subsequent reaction to form a metal sulphide salt may be represented by the following chemical equations:

$$H_2S\,(aq) \leftrightarrow\ HS^-\,(aq) + H^+(aq) \qquad 3.1$$

$$HS^-\,(aq) + H^+\ \leftrightarrow\ S^{2-}\,(aq)\ + 2H^+(aq) \qquad 3.2$$

$$M^{2+}\,(aq) +\ HS^-\,(aq)\ \leftrightarrow MS(s) +\ H^+\,(aq) \qquad 3.3$$

Supersaturation is not solely dependent on pH. Various factors such as reagent concentration, metal to sulphide molar ratio and hydrodynamic conditions influence the supersaturation of a system. Chiang and co-workers (2007) studied the influence of different mixing configurations on supersaturation and product particle size distribution. They found that in the absence of micromixing, a wide particle size distribution was achieved due to different regions of supersaturation within the reactor. In the presence of micromixers, a narrow particle size distribution was observed. Larger mean particle sizes were observed in the absence of micromixing due to regions of low local supersaturation in the reaction zone.

Mokone and collaborators (2010) investigated the effect of metal to sulphide molar ratio on supersaturation and mean particle size of precipitates, particularly in the presence of excess sulphide at a constant pH. They observed a large number of fine copper sulphide particles with a highly negative surface charge in the presence of excess sulphide (metal to sulphide ratio < 1) at pH 6. The highly negative surface charge of the copper sulphide particles, in the presence of excess sulphide, was due to the absorption of H_2S, HS^- and S^{2-} on the particle surface (Kolthoff & Moltzau, 1935) (as cited by Mokone et al, 2010).

Typically, controlling supersaturation in metal sulphide precipitation processes is challenging. This is due to the high affinity between reactants which results in fast

reaction kinetics and nucleation rates. Consequently, the formation of fine particles is unavoidable. Owing to this, there is a need to investigate post precipitation techniques that may be used to induce aggregation of metal sulphide fines.

3.2 Aggregation inducing techniques

According to Hartel et al (1986) aggregation in a colloidal suspension may be induced by reducing the electrostatic repulsive force between particles. A reduction in the electrostatic repulsive force will change the surface charge of a particle and ultimately its surface properties. The development of charge on a metal sulphide surface interface is dependent on the aqueous solution composition (Bebie et al, 1998). This is due to the absorption of potential determining ions on the particle surface. As a result, it is crucial to understand how the surface properties of metal sulphides, suspended in an aqueous solution, change when the composition of the bulk solution is altered.

3.2.1 Effect of solution chemistry on the zeta potential

Bebie and co-workers (1998) investigated the effect of pH and solution composition on the zeta potential of nickel sulphide (vaesite). In that study, a pH range between 2 and 8 was tested and 0.5 mmol of nickel ions were added to change the solution composition.

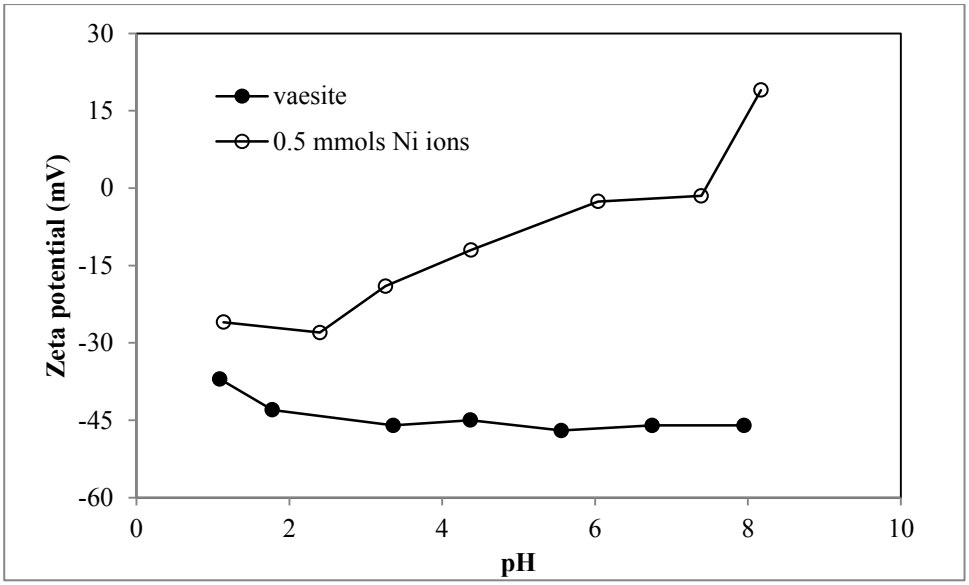

Figure 3.3: Effect of solution pH and excess nickel ions on the zeta potential of nickel sulphide (Bebie et al, 1998)

According to the results on Figure 3.3, increasing the solution pH from 2 to 4, increased the absolute magnitude of the zeta potential and resulted in highly negative zeta potential values. Beyond a pH of 4, further increasing the pH does not significantly change the zeta potential of suspended nickel sulphide particles. The addition of nickel ions resulted in a decrease in the absolute magnitude of the zeta potential for all the pH values tested. Subsequently, less negative zeta potential values were obtained. Bebie and collaborators (1998) further reported that at a pH of 8, aggregation of suspended colloids was observed in the presence of nickel ions.

In the same study, Bebie and co-workers (1998) conducted similar tests on an iron sulphide (pyrite) suspension. A pH range between 2 and 12 and the effect of sulphide ions on zeta potential was tested. Hydrogen sulphide was used as the sulphide ion source.

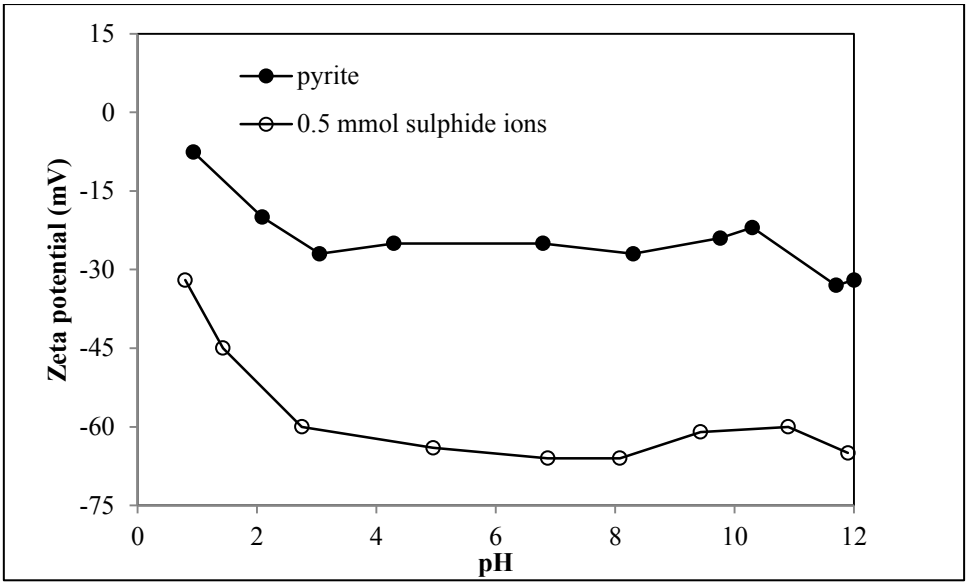

Figure 3.4: Effect of solution pH and excess sulphide ions on the zeta potential of iron sulphide (Bebie et al, 1998)

As can be seen from Figure 3.4, Bebie and collaborators (1998) observed similar trends between the pyrite and vaesite suspensions in the absence of excess ions. For a pyrite suspension, an increase in pH resulted in an increase in the absolute magnitude of the zeta potential within the range of pH values tested. The addition of 0.5 mmol of sulphide ions to the pyrite suspension resulted in a significantly lower zeta potential vs pH curve for pyrite. It follows that the presence of sulphide ions further increased the absolute magnitude of the zeta potential values, which resulted in highly negative zeta potential values for the pyrite suspension.

These results are in agreement with those obtained by Mokone and collaborators (2010) in a study that investigated the effect of solution pH and metal to sulphide molar ratios on the zeta potential of zinc and copper sulphide suspensions. Figure 3.5 illustrates the effect of solution pH on the zeta potential of both suspensions at a constant metal to sulphide molar ratio of 0.67 (in the presence of excess sulphide).

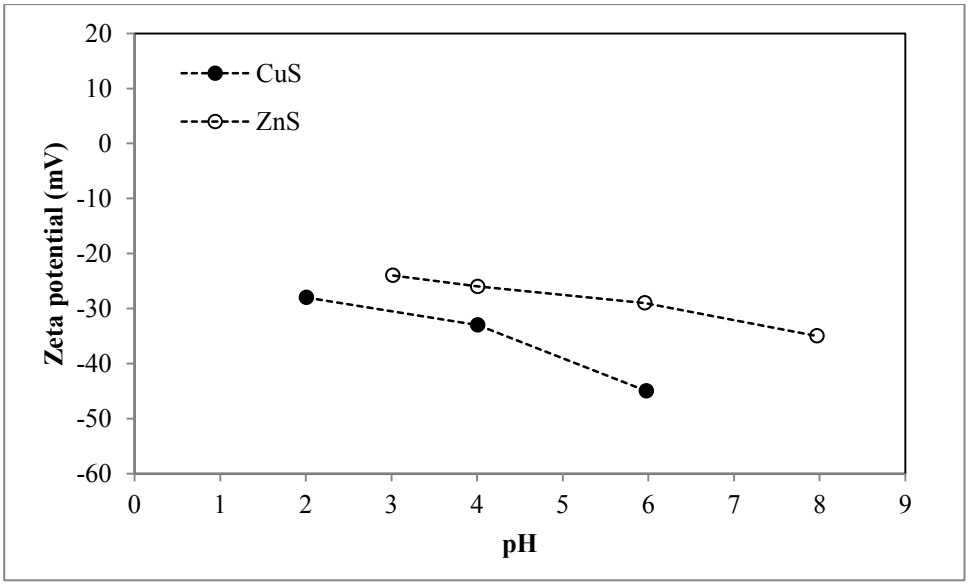

Figure 3.5: Effect of solution pH on the zeta potential of copper and zinc sulphide suspensions (Mokone et al, 2010)

As can be seen on Figure 3.5, the zeta potential values of both copper and zinc sulphide suspensions became more negative with increasing pH. Conversely, as the pH was decreased the zeta potential values of both suspensions became less negative. According to Figure 3.2, a reduction in pH results in a decrease in the amount of HS^- ions in solution (Kolthoff & Moltzau, 1935) (as cited by Mokone et al, 2010). As HS^- ions are potential determining ions and adsorb onto the surface of suspended particles, a decrease in the concentration of these ions further results in a less negative zeta potential. As the zeta potential of a suspension becomes less negative, aggregation between suspended particles becomes favourable.

The following metal to sulphide molar ratios were tested by Mokone and collaborators (2010):

Table 3.1: Metal to sulphide molar ratios tested

M:S molar ratio	Description	pH
2	Excess metal ions	6
1	Equimolar quantities	6
0.67	Excess sulphide ions	6

Figure 3.6 depicts the results obtained by testing the effect of metal to sulphide molar ratio on the zeta potential of copper and zinc sulphide suspensions.

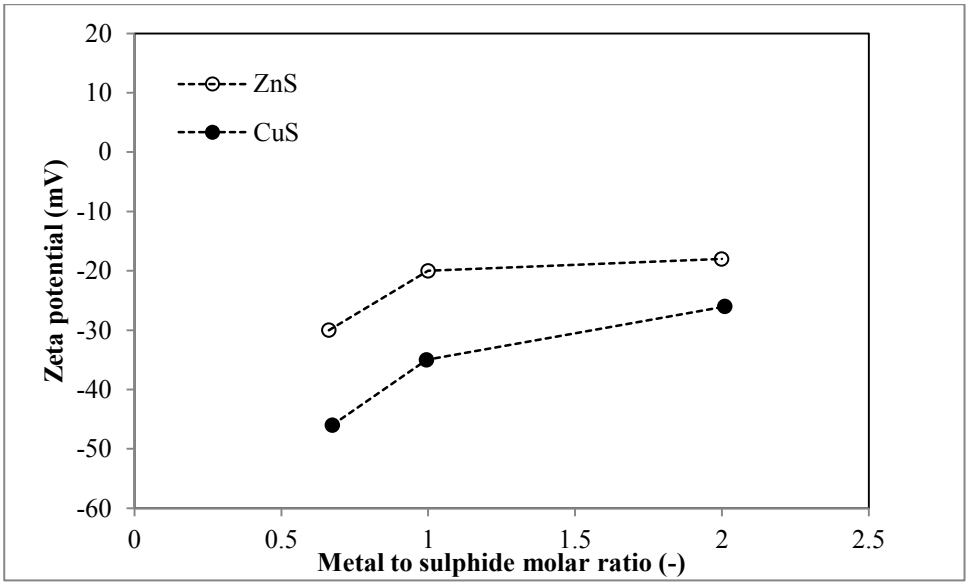

Figure 3.6: Effect of metal to sulphide molar ratio on the zeta potential of copper and zinc sulphide (Mokone et al, 2010)

As the metal to sulphide molar ratio was increased, the zeta potential values of both suspensions became less negative. Suspended zinc sulphide particles obtained a minimum zeta potential of - 16 mV when subjected to excess zinc ions. This is considerably higher than the minimum reached by the copper sulphide suspension counter-part. Mokone and co-workers (2010) observed a larger mean particle size for zinc sulphide particles when compared with copper sulphide. As a result of both the less negative zeta potential values and larger mean particle size, the zinc sulphide suspension showed good settling characteristics for all the metal to sulphide molar ratios tested. In the presence of excess sulphide ions, the zeta potential values of both suspensions were highly negative due to the high concentration of potential determining ions. This result was predominantly observed in the case of copper sulphide. As a result, suspended copper sulphide particles are more likely to carry a significant surface charge and develop strong inter-particle repulsion forces. Consequently, Mokone and co-workers (2010) reported that in the presence of excess sulphide ions, copper sulphide particles exhibited poor settling characteristics.

Using the solution chemistry of a suspension as a tool to reduce inter-particle electrostatic repulsive has been used extensively over the years. Nduna and co-workers (2013) went a step further than the previously mentioned authors and measured the settleability of copper sulphide suspensions with varying zeta potential values. Settleability is a measure of the settled volume of suspended particles per Litre of suspension. This provides a direct link between zeta potential and settleability and validates whether a particular suspension obeys the DLVO theory. Moreover, in the study conducted by Nduna and collaborators (2013) the effect of the concentration of excess copper and sulphide ions on the zeta potential and settleability of suspended copper sulphide particles was testsed. This was done by varying the concentration of copper and sulphide ions between 15 mg/L and 25 mg/L and 7 mg/L and 12 mg/L respectively. A pH value of 6 was maintained for these experiments. As shown in Figure 3.7, the zeta potential and settleability of copper sulphide particles increased from initial values of - 50 mV and 7 mL/L to - 42.7 mV and 18 mL/L respectively when 15 mg/L of copper ions were added to the suspension. A maximum zeta potential of - 40 mV was attained when 25 mg/L of copper ions were added to the copper sulphide suspension. A settleability of 21 mL/L was measured for this suspension.

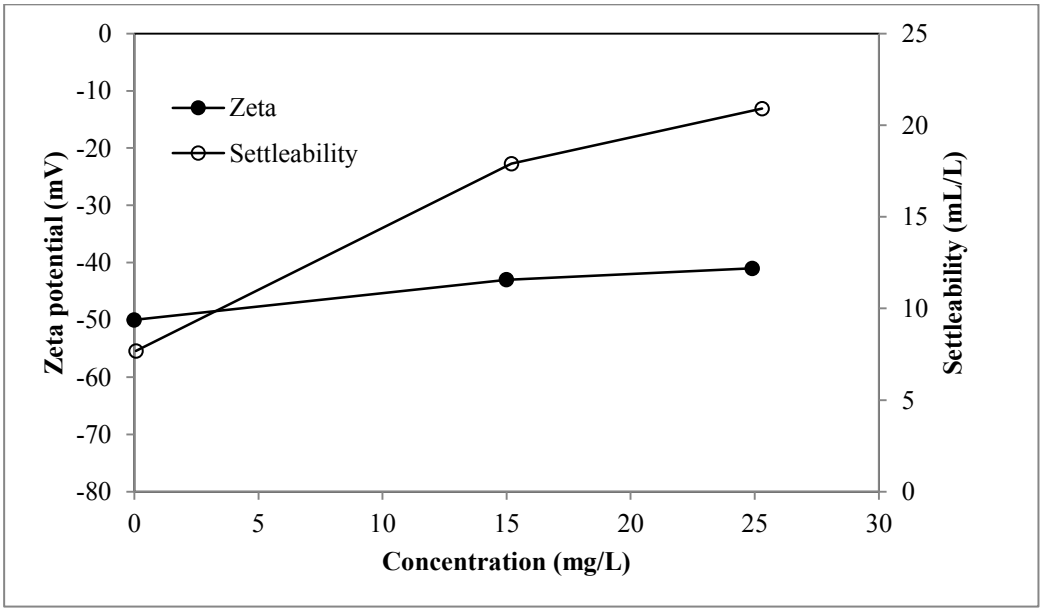

Figure 3.7: Effect of excess copper ions on the zeta potential and settleability of copper sulphide (Nduna et al, 2013)

From Figure 3.8, it is evident that increasing the concentration of sulphide ions, in a copper sulphide suspension, decreases both the zeta potential and settleability of the suspended particles. The zeta potential and settleability of copper sulphide particles decreased from initial values of - 50 mV and 7 mL/L to - 57.2 mV and 0 mL/L respectively when 7 mg/L of sulphide ions were added to the suspension. Increasing the concentration of sulphide ions to 12 mg/L further decreased the zeta potential and had no effect on settleability as it had already been reduced to 0 mL/L.

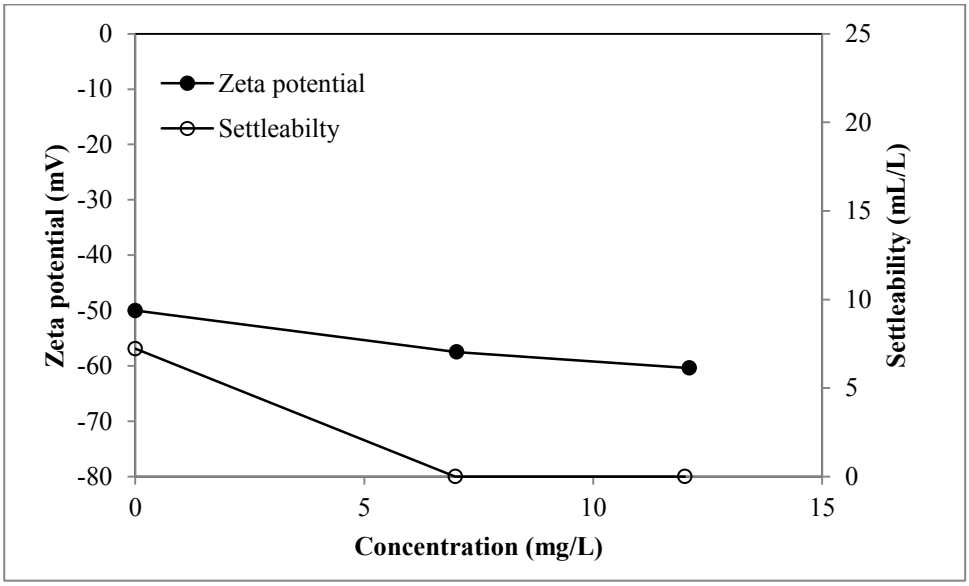

Figure 3.8: Effect of excess sulphide ions on the zeta potential and settleability of copper sulphide (Nduna et al, 2013)

Bebie and co-workers (1998), Mokone and collaborators (2010) and Nduna and colleagues (2013) all observed similar trends on the effect of solution chemistry on zeta potential, for various metal sulphide suspensions. Dekkers and Schoonen (1994) (as cited by Nduna et al, 2013) summarized the effect of metal sulphide lattice ions on zeta potential as follows: an increase in the metal ions results in an increase in the zeta potential (less negative zeta potential) and an increase in the sulphide ions results in a decrease in the zeta potential (more negative zeta potential).

3.2.2 Effect of ionic strength on zeta potential

As the electrical double layer is strongly affected by ionic strength, variations in the ionic strength of an aqueous medium affect the particle zeta potential. Vergouw and co-workers (1998) investigated the effect of ionic strength on the zeta potential and settling velocity of lead sulphide (galena) and iron sulphide (pyrite). The ionic strength was increased by adding 60 ppm of calcium ions to the respective suspensions. For galena, they found that an increase in the ionic strength increased both zeta potential and settling velocity. According to Vergouw and collaborators (1998) this increase in zeta potential indicates the adsorption of positive calcium ions on the particle surface. This resulted in a less negative zeta potential. An increase in the settling velocity of galena indicates aggregation of galena particles. Tests conducted on the pyrite suspension showed that in the presence of calcium ions, the zeta potential increased. However, the settling velocity of pyrite was lowered when calcium ions were added to the suspension.

Mokone and co-workers (2012) also investigated the effect of ionic strength on the zeta potential of copper and zinc sulphide. In that study, the effect of both divalent and trivalent ions on zeta potential was tested. Calcium and aluminium ions were used as the source of divalent and trivalent ions respectively. According to Mokone and collaborators (2012) increasing the ionic strength by adding calcium ions had little effect on the zeta potential of both copper and zinc sulphide suspensions resulting in a slight increase in zeta potential. In contrast, a different result was seen when 0.5 mmol of aluminium ions were added to both suspensions. The zeta potential of copper sulphide particles increased from an initial value of - 30 mV to - 10 mV in the presence of aluminium ions. Similarly, an increase in zeta potential of zinc sulphide particles was also observed from an initial value of - 25 mV to - 5 mV. According to Goodwin (1982) (as cited by Nduna, 2013) zeta potential values in the range - 15 mV to 15 mV correspond to minimum repulsion between suspended particles. Subsequently, aggregation of suspended particles was observed in both cases.

The results obtained by Vergouw and co-workers (1998) and Mokone and collaborators (2012) are comparable. Both studies showed that increasing the ionic strength of the bulk solution results in a less negative zeta potential and enhanced settling characteristics of various metal sulphide suspensions.

3.2.3 Effect of partial oxidation on zeta potential

According to Fullston and co-workers (1999) the surface of sulphide minerals is very reactive and starts to oxidise as soon as the mineral is in contact with water. Oxidation can reverse the sign and change the magnitude of the zeta potential of a sulphide mineral. Consequently, metal sulphides are sensitive to surface oxidation. Bebie and collaborators (1998) investigated the effect of surface oxidation on pyrite. This was done by determining and comparing the pH dependence of the zeta potential of pyrite in both an oxygen abundant and deficient (under nitrogen) environment.

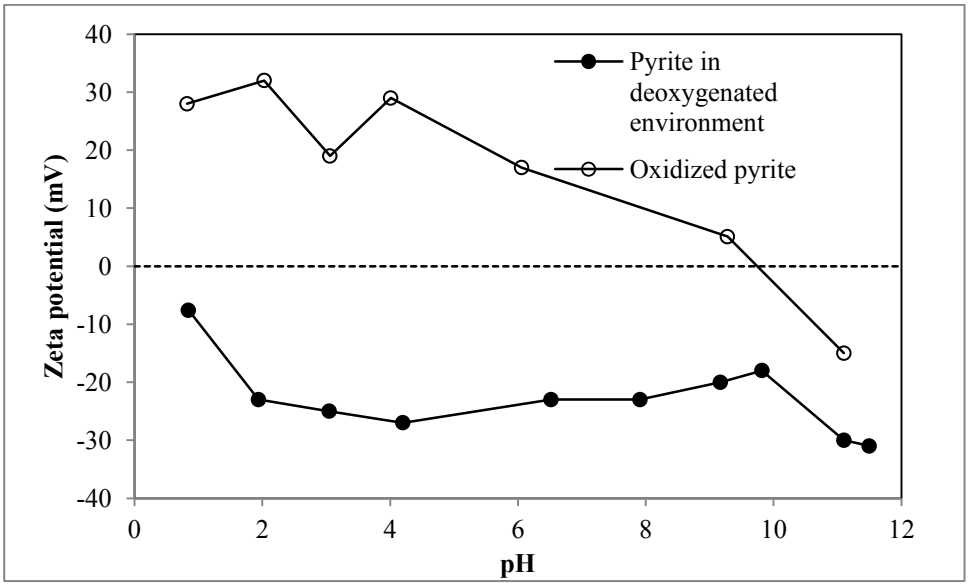

Figure 3.9: pH dependence of zeta potential in oxygen abundant and deficient environment for a pyrite suspension (Bebie et al, 1998)

As can be seen on Figure 3.9, a comparison between the two plots shows that in an oxygen abundant environment, the iso-electric pH (also known as the point of zero charge) of pyrite shifts from < 2 to approximately 9.5. The zeta potential of pyrite in an oxygen deficient environment is highly negative. This is comparable to that of elemental sulphur or a sulphide mineral with a sulphur rich surface (Bebie et al, 1998; Fullston et al 1999).

Nduna (2013) investigated the effect of partial oxidation on the zeta potential and settleability of a copper sulphide suspension at a constant pH of 6. Moreover, in that

study the effect of varying oxygen exposure time was tested. As can be seen on Figure 3.10, an increase in both the zeta potential and settleability was observed with increasing oxygen exposure time. This was due to a higher extent of oxidation with increasing exposure time. The settleability of the copper sulphide suspension increased from an initial value of 7 mL/L to a maximum of 27 mL/L for an exposure time of 60 minutes.

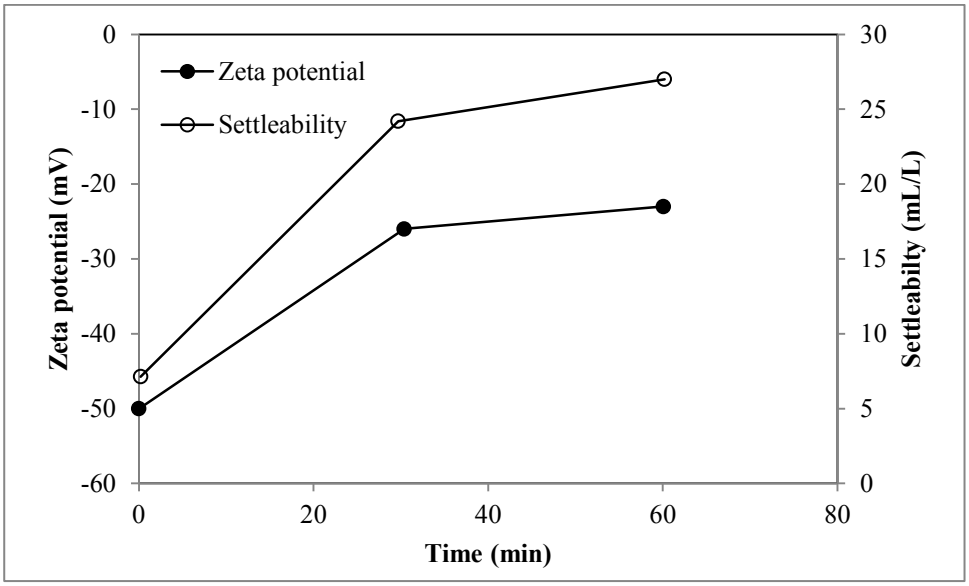

Figure 3.10: pH dependence of zeta potential and settleability in an oxygen abundant environment for a copper sulphide suspension (Nduna, 2013)

The oxidation of a sulphide mineral surface in water proceeds via the following reaction (Fullston et al, 1998):

$$MS + \frac{1}{2}n\,O_2 + n\,H_2O \rightarrow M_{1-n}S + nM(OH)_2 \qquad 3.4$$

Fornasiero and co-workers (1992) (as cited by Fullston et al, 1999) reported that when a sulphide mineral is exposed to oxygen, its surface charge becomes less negative and may even develop a positive charge. This is due to the formation of a metal hydroxide layer on the sulphide mineral surface.

Although the zeta potential of metal sulphides may be increased by oxidation, it is crucial to control the surface oxidation of these surfaces, as heavily oxidising them may form a coat of metal hydroxides which reduce the purity of metal sulphides.

3.3 Magnetic flocculation of ferromagnetic suspensions

Particle aggregation induced by a magnetic field is commonly referred as magnetic flocculation. According to Svoboda (1982), Parker and co-workers (1982) and Wang and collaborators (1994) particle flocculation occurs when a suspension of ferromagnetic mineral particles is exposed to a magnetic field and the magnetic dipole-dipole interaction between the particles is strong enough to outweigh the stabilising electrical double layer forces. This magnetic dipole-dipole interaction may result from an induced or permanent magnetic moment. Consequently, suspension stability may be reduced and aggregation of suspended particles may be achieved using this technique. However, effective aggregation is dependent on factors such as magnetic field strength and magnetic exposure time.

3.3.1 Extended DLVO theory

Svoboda (1982) proposed that the DLVO theory could be extended to include in addition to the van der Waals and double layer interaction terms, a magnetic dipole-dipole interaction. For the extended DLVO theory, the total potential interaction energy between particles is defined as follows:

$$V_T = V_R + V_{vdW} + V_m \tag{3.5}$$

$$V_m = -\frac{32\,\pi^2 a^6 \chi^2 {B_0}^2}{9\mu_0 r^3} \tag{3.6}$$

Where V_m is the magnetic dipole-dipole interaction, X is the magnetic susceptibility of the particle, B_o is the magnetic induction and μ_o is the magnetic permeability of a vacuum.

This magnetic dipole-dipole interaction acts as an attractive magnetic potential between particles. For ferromagnetic particles, this potential will always be dominant, due to the high magnetic susceptibility of such particles. The addition of this potential and the van der Waals force may eliminate the energy barrier prohibiting aggregation of particles.

3.3.2 Effect of magnetic field strength on magnetic flocculation of ferromagnetic suspensions

Wang and co-workers (1994) investigated the effect of magnetic field strength on the settled weight of hematite and chromite suspensions. In that study, the magnetic field strength was varied from 0 T to 2.15 T. Both suspensions were maintained at a constant pH of 8. As can be seen on Figure 3.11 the settled weight of hematite increased with increasing magnetic field strength. A significant change in settled weight was observed between 0 T and 0.65 T. Further increasing the magnetic field strength resulted in a smaller change in the settled weight of hematite. Figure 3.12 illustrates the effect of magnetic field strength on the settled weight for a chromite suspension. Similarly, increasing the magnetic field strength increased the settled weight of a chromite suspension. However, for a chromite suspension the biggest change in settled weight was observed between 1 T and 2 T.

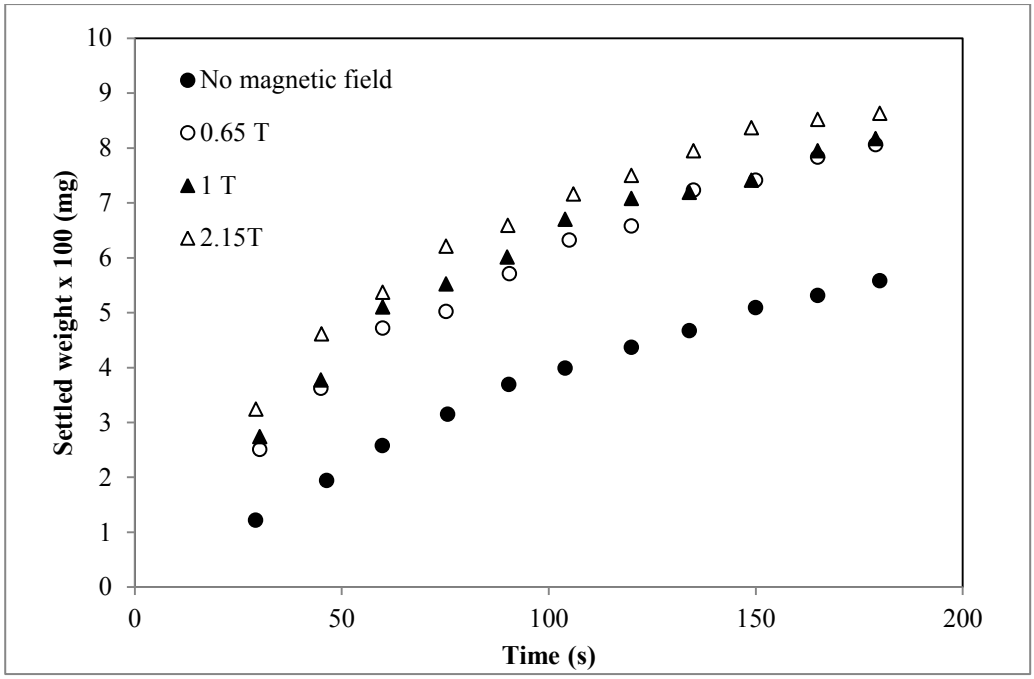

Figure 3.11: Effect of magnetic field strength on settled weight of hematite (Wang et al, 1994)

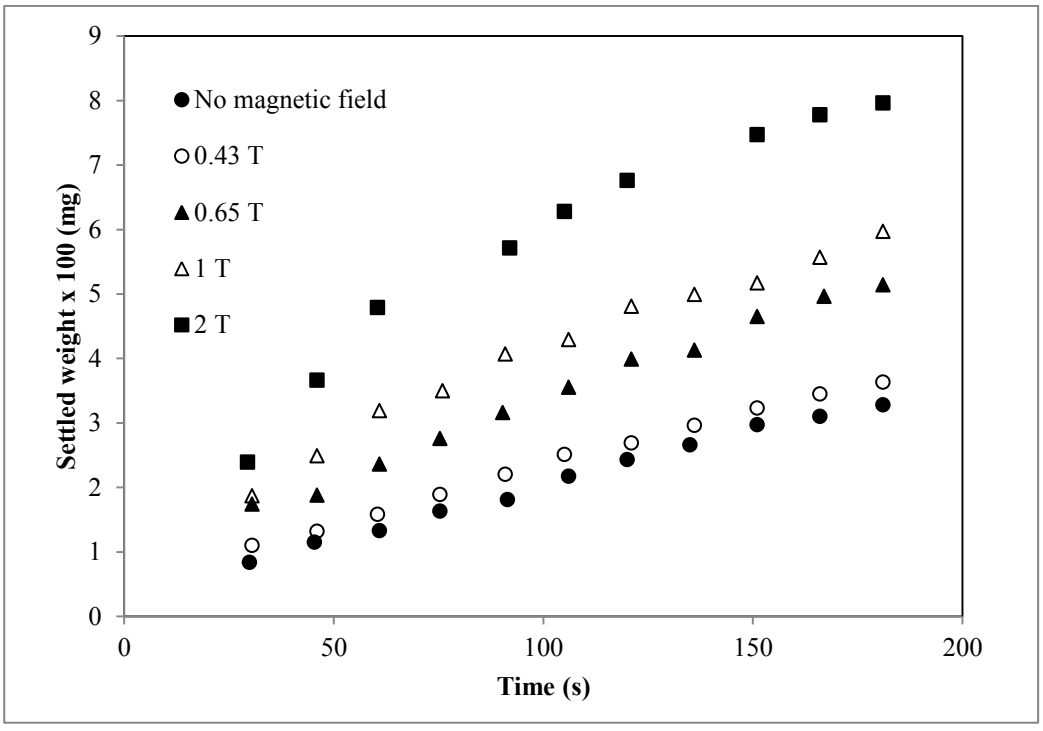

Figure 3.12: Effect of magnetic field strength on settled weight of Chromite (Wang et al, 1994)

Furthermore, a magnetic field strength of 0.43 T has negligible effect on the settled weight for a chromite suspension and therefore a minimum magnetic field strength of 0.65 T is required in order to achieve an appreciable settled weight.

The results obtained by Wang and co-workers (1994) are consistent with those reported by van Kleef and collaborators (1982) in a study on the sedimentation of colloids in high magnetic fields. In that study, the effect of magnetic field strength on the settling velocity of hematite was investigated in three magnetic field strength regions (low, intermediate and high). As can be seen on Figure 3.13, magnetic field strength has a linear relationship with settling velocity. As a result, increasing magnetic field strength increases the settling velocity of hematite.

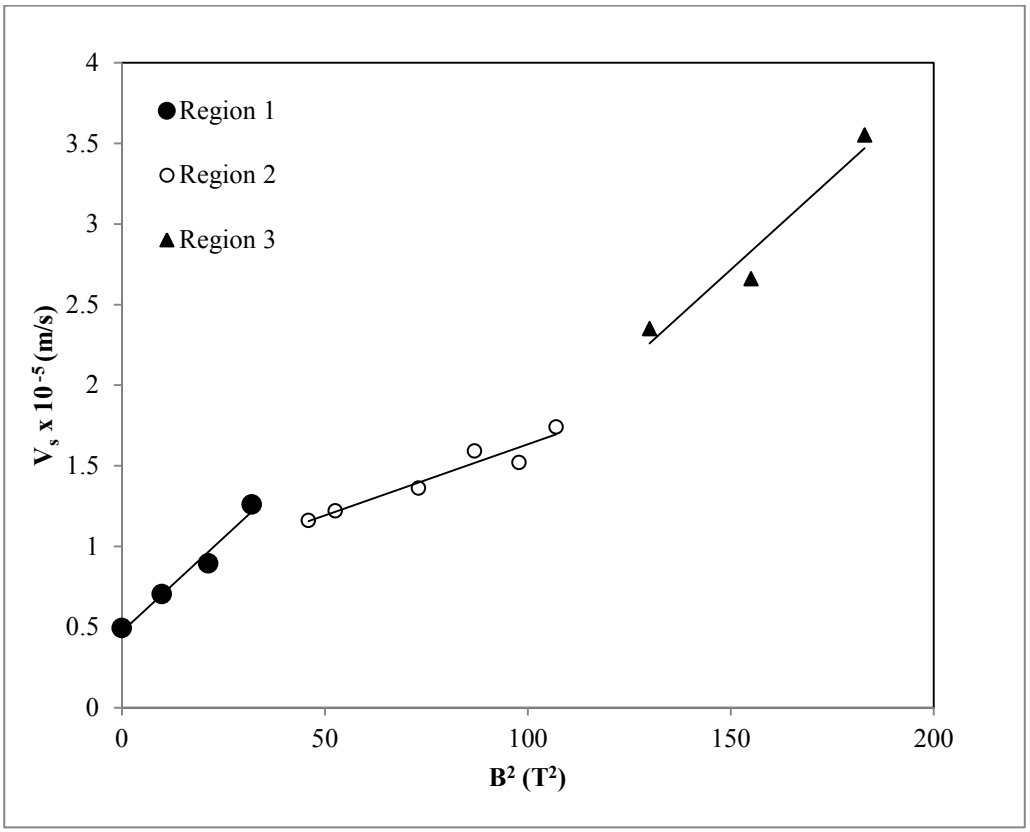

Figure 3.13: Effect of magnetic field strength on settling velocity of hematite (van Kleef et al, 1982)

In that study, van Kleef (1982) also observed an increase in the settling velocity of chromium and manganese oxide suspensions, with increasing magnetic field strength.

According to equation 3.6, magnetic field strength and magnetic susceptibility have a positive relationship with the magnetic dipole-dipole interaction. Consequently, an increase in the magnetic field strength should result in an increase in the settled weight/ settling velocity of ferromagnetic particles.

3.3.3 Effect of exposure time on magnetic coagulation of ferromagnetic suspensions

The duration a suspension spends in a magnetic field influences settling. Wang and co-workers (1994) investigated the effect of magnetic exposure time, on the settled weight of hematite and chromite suspensions, at constant magnetic field strengths. The results can be seen on Figures 3.11 and 3.12 for hematite and chromite respectively. Each curve represents the effect of exposure time on settled weight, for a specified magnetic field strength. For both the hematite and chromite suspensions increasing exposure time, at a constant magnetic field strength, resulted in a higher settled weight. This was the anticipated result as increasing exposure time allows more time for inter-particle interaction and therefore increases the likelihood of inducing aggregation.

3.4 Magnetic water treatment

In industry, magnetic water treatment is widely applied as an antiscale treatment method. However, in literature the effectiveness of magnetic water treatment for scaling remediation is considered controversial as contrasting theories on the mechanism behind it have been presented (Baker & Judd, 1996; Parsons et al, 1997). Sohnel and Mullin (1988) (as cited by Baker & Judd, 1996) demonstrated that the homogenous nucleation rate of calcium carbonate would remain unchanged by a 0.5 T magnetic field. Contrary to findings by Sohnel and Mullin (1988), Baker and Judd (1996) reported reduced nucleation rates for calcium carbonate and calcium sulphate in the presence of a 0.7 T magnetic field. Figure 3.14 below, depicts the results obtained by Baker and Judd (1996).

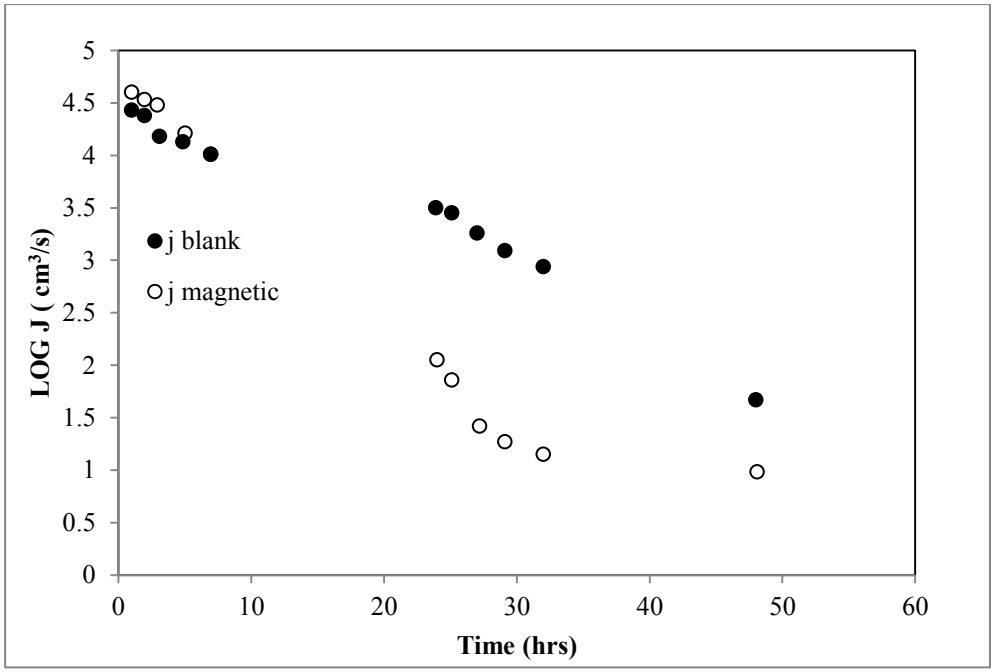

Figure 3.14: Effect of magnetic field on the nucleation rate of calcium carbonate (Baker & Judd, 1996)

It is clear that there are competing theories on the effect of a magnetic field on crystallization particle rate processes. However, the application of a magnetic field post precipitation may still be explored.

3.4.1 Lorentz ion shift effect on zeta potential

According to Gamayunov (1983) (as cited by Kozic & Lipus, 2003), Lipus and co-workers (2001) and Velev and Bhatt (2006) the zeta potential of a particle can be altered by the application of an external field. This is because, when colloids in solution are exposed to a magnetic field, a Lorentz force is created which acts on every charged particle moving through the field as shown in equation 2.21.

Gamayunov (1983) was the first to develop a model for the possible effect of a magnetic field on the electrical double layer. This model suggested that a Lorentz force may disturb the equilibrium of ions in the diffuse layer by possible displacement of co and counter-ions. This would result in a change in the charge distribution within the electrical

double layer and therefore alter the electric potentials of the stern layer and slipping plane.

In a study on amelioration of dispersion separations in order to control scale formation Lipus and co-workers (2001) expanded the ideas of Gamayunov (1983) and suggested that the Lorentz force results in the shifting of ions in the bulk solution and close to the particle surface and may therefore disturb ions in both the diffuse and Stern layers. However, this ion shift is retarded by the liquid viscosity force. The viscosity force is equal to the Lorentz force in accordance with Newton's law for force balance. As a result, the Lorentz ion shift, Δx_i, is derived from this relationship via equation 2.21 and 3.7:

$$F_{vis} = \frac{-6\Pi\eta a_i \Delta x_i}{t} \qquad 3.7$$

Where F_{vis} is the liquid viscosity force, η is the fluid viscosity, *t* is the exposure time and Δx_i is the Lorentz ion shift.

$$\Delta x_i = \frac{q}{6\Pi\eta r_i} Btv \qquad 3.8$$

Calculation of the Lorentz ion shift for ions in the bulk solution revealed that the Lorentz force has very little or no effect on the collision probability of these ions. However, the Lorentz ion shifts become significant close to the particle surface. Lipus and co-workers (2001) reported that shifted counter-ions in the Stern layer will remain adsorbed for a longer time according to desorption time estimations for bivalent ions of natural waters. This is because these bivalent ions have high desorption energies. Without strong adsorption of the shifted counter-ions in the Stern layer and electrostatic attractions, this desorption time would be much shorter. The ion shifts by Lorentz force translates into successful charge destabilization close to the particle surface, alters the zeta potential of particles and thus enhances the settling characteristics of a suspension.

In that study, Lipus and co-workers (2001) showed that the application of a magnetic water treatment method post precipitation may be used to reduce the stability of calcium carbonate precipitates in industrial water processes.

3.4.2 Effect of particle speed on Lorentz force

A charged particle will experience a Lorentz force in the presence of a magnetic field, only if it is moving (Knight, 2008). Typically, particles in a suspension move around in Brownian motion. As a result, suspended particles will experience a Lorentz force when exposed to a magnetic field. The magnitude of this Lorentz force is dependent on the magnitude of the particle speed. An increase in particle speed will increase the Lorentz force acting on the particle. This is in accordance with equation 2.21.

3.5 Research motivation

3.5.1 Aim

This research was aimed at studying the settling rates of metal sulphides (which affect their gravitational separation efficiency) by investigating the effect of a magnetic field on zeta potential, and thus on aggregation.

3.5.2 Objectives

The key objective was to study the effect of a magnetic field on the inter-particle electrostatic repulsive forces, which hinder aggregation, by measuring the zeta potential.

3.5.3 Hypotheses

The following hypotheses were made:

1. Exposing a metal sulphide suspension to a magnetic field will reduce repulsive electrostatic forces between suspended particles. This reduction in repulsive electrostatic forces, is due to an increase in the Lorentz ion shift and will be indicated by a less negative suspension zeta potential.

2. Increasing the exposure time at a constant magnetic field strength will result in a decrease in electrostatic repulsive forces between particles.

3.5.4 Key questions

The following key questions were developed from the objectives:

1. What effect does the magnetic field strength have on the zeta potential of a suspension at constant exposure time?
2. Is there a threshold magnetic field strength that must be achieved for a change in zeta potential at constant exposure time?
3. What effect does the exposure time have on the zeta potential of a suspension at constant field strength?
4. What effect does the suspension velocity have on the zeta potential at constant magnetic field strength and charge?

4. Methodology

As this study focussed on a post precipitation step, it necessitated the precipitation of copper sulphide colloids as a prerequisite. This resulted in a two- step experimental design. The first step included the precipitation of a copper sulphide suspension and subsequent analytical analysis. While the second step involved the application of a magnetic field to the colloids precipitated in the first step and further analytical analysis.

4.1 Metal sulphide precipitation

4.1.1 Chemical reagents

The following chemical reagents were used for the experiments conducted in this study, copper sulphate pentahydrate, sodium sulphide nonahydrate, sodium hydroxide and sodium chloride. All the above listed reagents were of analytical grade from Sigma-Aldrich. For the purposes of this work, 99.99 % nitrogen gas from Afrox Industrial Gases was used.

4.1.2 Experimental setup

Two closed 4 L glass vessels were used as storage tanks for the bulk sodium sulphide and copper sulphate aqueous solutions. A T-mixing device comprising of two inlet ports, a mixing channel and an outlet port was used. This device was connected to a magnetic gear pump (Micropump®; 1-Drive; 76003) which provided the suction required to move the reacting reagents from the storage tanks to the T-mixer. A 1 L glass vessel was used as a collection vessel for the copper sulphide suspension outflow from the T-mixer. Plastic tubes 4mm in diameter were used to transport each reagent from its storage tank to the respective T-mixer inlet port and from the T-mixer outlet port to the suspension collection vessel. The reaction occurred as soon as the reagents came into contact and further proceeded in the tube connected to the outlet port. The experimental setup is depicted in Figure 4.1.

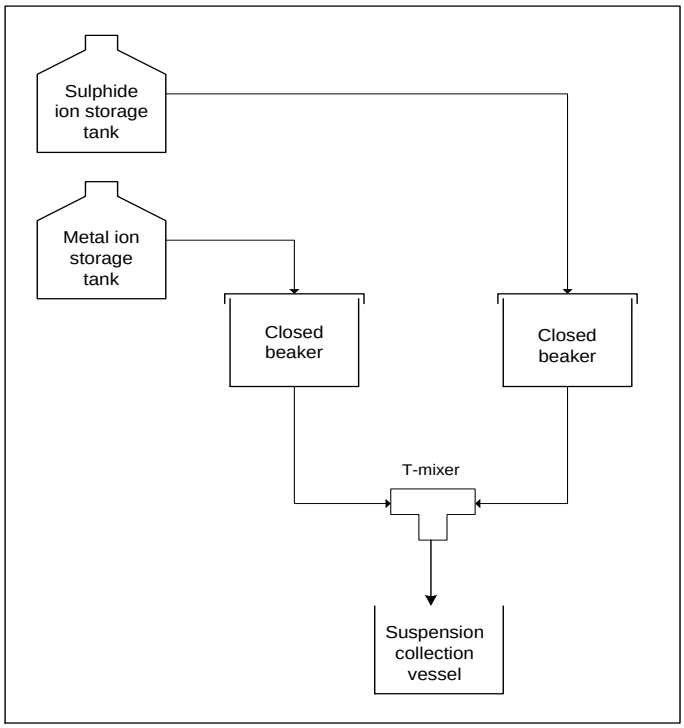

Figure 4.1: T-mixer setup for the precipitation of a copper sulphide suspension

4.1.3 Experimental procedure

The precipitation step was carried out at atmospheric pressure and 23 ˚C ± 2 ˚C. A metal ion solution with a concentration of 500 mg/L was prepared by dissolving copper sulphate pentahydrate in de-ionised water. After which, a sodium sulphide solution equi-molar to the metal ion solution was prepared by dissolving sodium sulphide nonahydrate in de-ionised water. Both solutions were stored in 4L bulk closed vessels as bulk solutions.

For each experimental run, 500 mL of the metal and sulphide ion solutions were poured into separate beakers. 2 mL of a 1M sodium hydroxide solution was pipetted into the beaker containing sodium sulphide to maintain the pH of the copper sulphide solution formed at a value above 6. This was done to limit the formation of hydrogen sulphide gas, which may form at pH values below 6. The addition of this constant volume of sodium hydroxide also helped maintain a constant pH for each experimental run. Each beaker was closed off with a layer of parafilm. A 4mm diameter hole was made in each

parafilm layer to provide access to the solution inside each beaker. 200 mL of a 0.01 M sodium chloride solution was poured into a volumetric flask. This solution together with both the metal ion and sulphide ion solutions in their respective beakers were sparged with nitrogen gas. This was done to limit oxidation of the reacting reagents and the sodium chloride spectator ions used during sampling. For each run, all the reagents were sparged for 20 minutes. After sparging, the reaction proceeded in a T-mixing device supplied with reactants by a magnetic gear pump. For effective mixing in a T-mixer, a Reynolds number in the turbulent region must be maintained (Weigl, 2003). This corresponds to a pump speed equal to or greater than 1427 rpm. Consequently, for each experimental run a pump speed greater than 1427 rpm was used. Due to equipment limitations, a constant pump speed for each experimental run could not be maintained. However, the pump speed was recorded for each experimental run and overall a range between 1650 rpm and 2885 rpm was used. A 1L glass vessel was placed at the output end of the T-mixer to collect the formed copper sulphide suspension. From this vessel, a sample of the suspension was taken in order to measure the zeta potential straight after precipitation.

For sampling, a 10 mL syringe was filled with the copper sulphide suspension. This was then dispensed into a 42 mL sample bottle already containing 32 mL of sodium chloride spectator ions with an ionic strength of 0.01 M. The zeta potential of the sample was then measured. Once the zeta potential had been measured, the copper sulphide suspension was exposed to a magnetic field.

4.2 Magnetic exposure of metal sulphide suspension

4.2.1 Chemical reagents

No chemical reagents were used for this step.

4.2.2 Experimental setup

A Magnetometer was used to generate the magnetic field required in this study. This magnetometer was set up in the catalysis laboratory and consisted of two unlike magnetic poles, a sample holder between the poles, a central control computer and an

electric motor system. The magnetometer could achieve a maximum field strength of 2 T. The magnetometer setup is depicted in Figure 4.2.

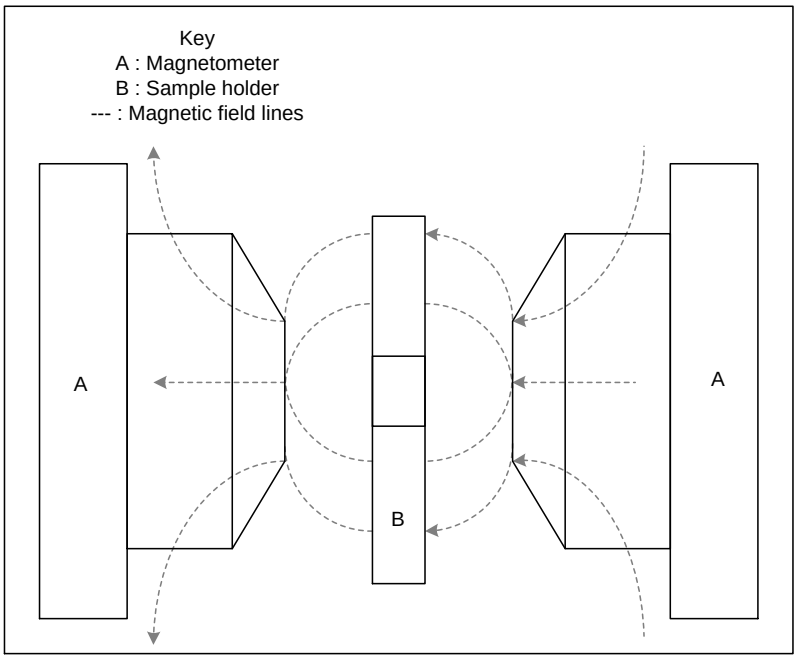

Figure 4.2: Schematic of magnetometer

4.2.3 Experimental procedure

For this step, a cuvette with a volume of 2 mL was filled with the suspension. The cuvette was then placed in the middle of a 30 cm long stainless steel cylindrical sample holder with a diameter of 1.27 cm. At this midpoint, the cuvette is exposed and not encased by the sample holder as there is a rectangular cut out. The sample holder was then placed between the two magnetic poles. This was a fixed position as the sample holder was screwed into the same position each time. Once the sample was in place, the magnet was switched on to the desired field strength for a set exposure time. For oscillating sample tests, the sample holder motor was switched on. The motor had a fixed speed of 2 Hz. The following field strengths and exposure times were tested:

Table 4.1: First set of experiments conducted

Sample type	Magnetic field strength [T]	Exposure time [min]
Non oscillating sample	0.5	40
	0.6	
	0.7	
	0.8	
	0.9	
	1	

Table 4.2: Operating conditions for magnetic exposure

Sample type	Magnetic field strength [T]	Exposure time [min]
Non oscillating sample	1	10
		20
		40
	1.5	10
		20
		40
	2	10
		20
		40
Oscillating sample	1	10
		20
		40
	1.5	10
		20
		40
	2	10
		20
		40

Subsequent to magnetic field exposure, the suspension zeta potential was measured once again.

4.3 Analytical techniques

4.3.1 Zeta potential

The Malvern Zetasizer Nano ZS was the instrument used to measure zeta potential. This machine uses a dynamic back light scattering technique for zeta potential measurements.

5. Results & discussion

5.1 Metal sulphide precipitation

Each precipitated copper sulphide suspension had an initial zeta potential equal to or less than - 40 mV. Mokone and co-workers (2010) and Nduna and collaborators (2013) reported that the zeta potential value of a copper sulphide suspension becomes more negative with increasing pH. Furthermore, Nduna and co-workers (2013) attained a zeta potential value of - 50.1 mV for a copper sulphide suspension precipitated at pH 9. Accordingly, this result was anticipated as each suspension was precipitated at a pH value of 6.3.

5.2 Magnetic coagulation of diamagnetic suspensions

This section details the results obtained by exposing suspended copper sulphide particles to a magnetic field.

5.2.1 Threshold field strength and exposure time required to modify zeta potential

Results from the first set of experiments listed in Table 4.1 are shown in Figure 5.1. This Figure illustrates that the change in zeta potential of copper sulphide suspensions at all the field strengths tested, with the exception of 1 T, in the first set of experiments is below 1 mV. It follows that, the magnetic field generated at field strength values less than 1 T had negligible effect on the change in the zeta potential of copper sulphide suspensions at a constant exposure time of 40 minutes.

At 1 T, there is a noticeable change in the zeta potential of a copper sulphide suspension from an initial value of - 40 mV to - 36 mV. This resulted in a slightly less negative zeta potential value.

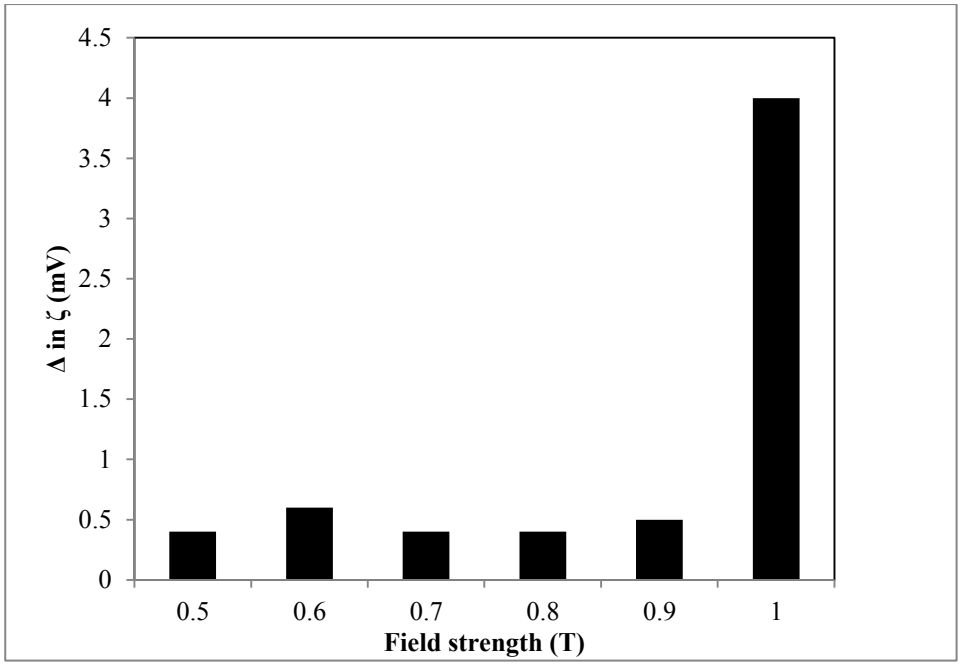

Figure 5.1: Change in zeta potential for a constant exposure time at various magnetic field strengths

The DLVO Theory states that a reduction in repulsive electrostatic forces yields a negative interaction energy which indicates that attractive forces dominate (Derjaguin et al, 1987; Schneider et al, 2011; Nduna, 2013).

As copper sulphide suspensions obey the DLVO Theory, the attractive van der Waals force and repulsive electrostatic force were calculated using equations 2.16 and 2.17 respectively. A Hamaker constant of 4 x 10^{-19} J (Horzempa & Helz, 1979) (as cited by Nduna, 2013) and an average particle radius of 5 nm was used to determine the van der Waals potential. From this calculation, the net interaction energy for both the initial and final zeta potential values was plotted. These plots can be seen on Figures 5.2 and 5.3.

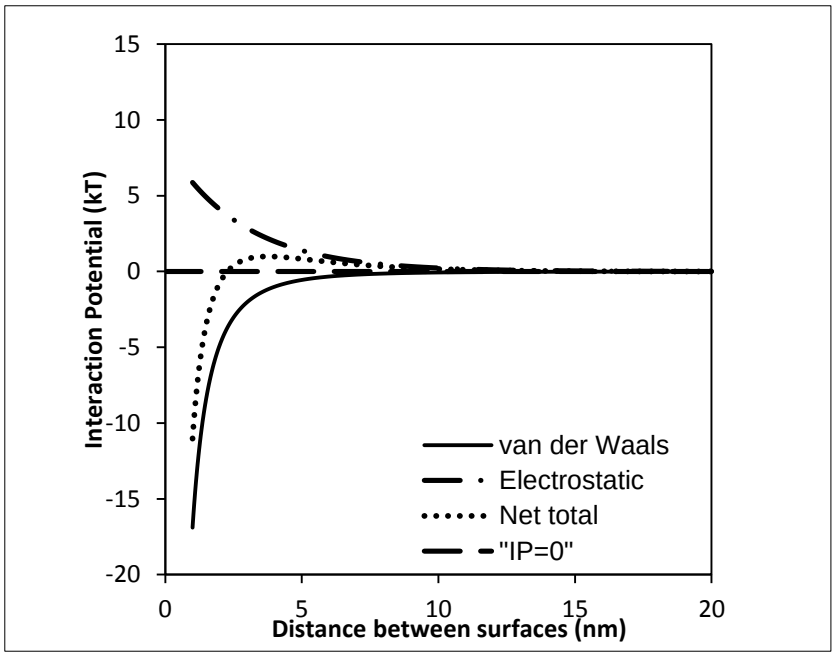

Figure 5.2: Net interaction energy plot for a suspension with a zeta potential of - 40 mV

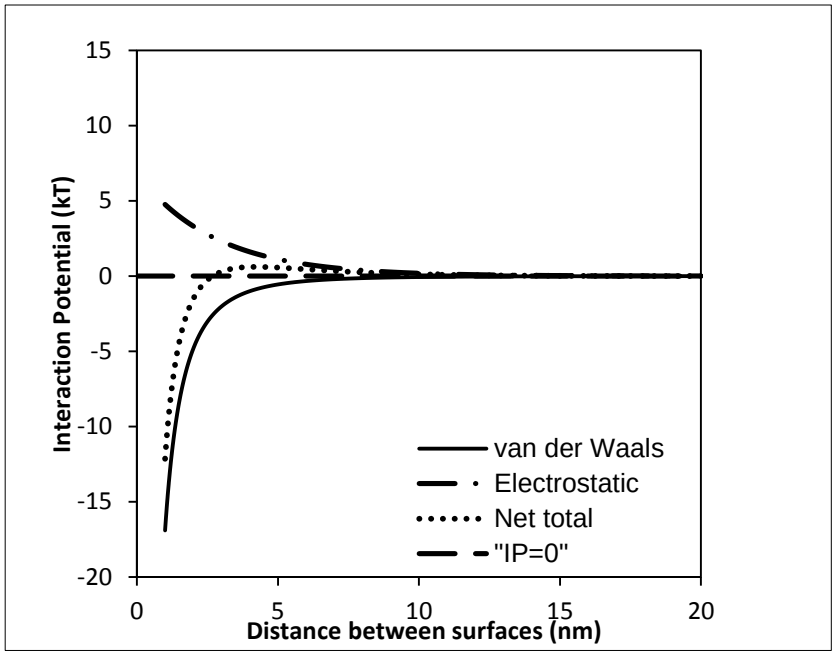

Figure 5.3: Net interaction energy plot for a suspension with a zeta potential of - 36 mV

A comparison of the net interaction plots illustrated on Figures 5.2 and 5.3 showed that the maximum net interaction energy was reduced from 0.99 kT to 0.61 kT for a

suspension with initial and final zeta potential values of - 40 mV and - 36 mV respectively. This is indicated by the lower absolute maximum on Figure 5.3. Moreover, this decrease translated to a reduction in the electrostatic repulsive force between colloids. This reduction is not enough to increase the settling kinetics of the particles significantly. This is because a suspension with an average particle size greater than 3.5 nm and a zeta potential value of - 36 mV is still within the stable colloid range with a positive net interaction energy which indicates that repulsive electrostatic forces dominate.

5.2.2 Effect of magnetic field strength on zeta potential

The effect of magnetic field strength on the zeta potential of a copper sulphide suspension was investigated in the second set of experiments (Table 4.2). Figure 5.4 shows the effect of various magnetic field strengths on the zeta potential of suspended copper sulphide particles. The initial zeta potential of each suspension is shown at t = 0 minutes.

The results from this set of experiments showed that increasing magnetic field strength, while keeping the exposure time constant, increased the zeta potential. This result is supported by the three data points at t = 40 minutes. At high magnetic field strengths, a less negative zeta potential was obtained and therefore a greater increase in zeta potential was achieved. From Figure 5.4, a comparison between the initial and final zeta potential values at t = 0 and t = 40 minutes for suspensions exposed to 1 T, 1.5 T and 2 T showed that largest reduction in the absolute magnitude of the zeta potential was achieved at 2 T.

The highest magnetic field strength tested was 2 T. The largest reduction in zeta potential was seen at this field strength.

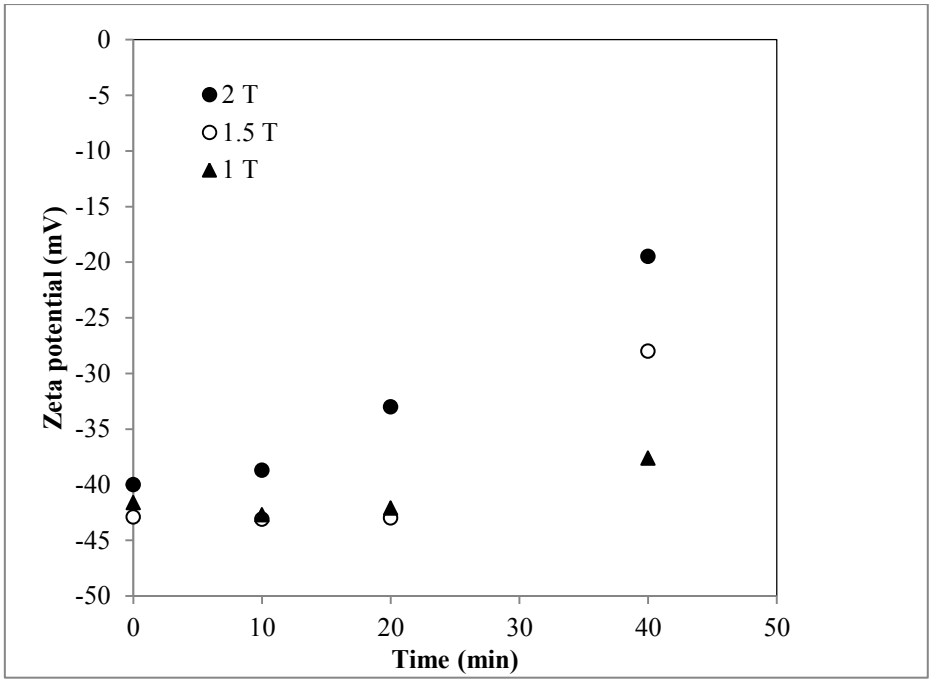

Figure 5.4: Zeta potential of copper sulphide as a function of exposure time at constant field strength

Changes in zeta potential observed when suspensions are exposed to a magnetic field are due to the Lorentz force effect on ions close to the copper sulphide particle surface (Lipus et al, 2001). This effect is commonly known as the Lorentz ion shift and is solely responsible for the changes in zeta potential observed in this study.

According to equation 2.21, the Lorentz force increases with increasing magnetic field strength at constant charge and particle velocity. This is why greater changes in the zeta potential of copper sulphide suspensions are observed at higher field strengths. It is imperative to note that although magnetic exposure destabilizes charge close to the particle surface, the overall system charge remains electro-neutral.

5.2.3 Effect of exposure time on zeta potential

The relationship between magnetic field exposure time and zeta potential was tested at constant magnetic field strength. Figure 5.4 also shows the effect of exposure time on zeta potential. Each curve on this Figure depicts the effect of increasing exposure time, while maintaining a constant magnetic field strength, on the suspension zeta potential. The results showed that increasing the exposure time, at constant field strength, results in

a significantly less negative zeta potential and thus an increase in zeta potential. This result is supported by the positive slope of each curve on Figure 5.4. In addition to this, the rate at which the zeta potential increases is increased at higher field strengths. This is indicated by the steeper curve for the 2 T results and the higher zeta potential values obtained for each exposure time.

At 1 T, exposure times of 10 and 20 minutes seem to have no effect on zeta potential. This is because to observe a noticeable change in the zeta potential of a copper sulphide suspension, a threshold magnetic field strength of 1 T for an exposure time of 40 minute is required.

As can be seen on Figure 5.4, at 1.5 T, a negligible effect on the zeta potential was observed for exposure times of 10 and 20 minutes. However, for an increased exposure time of 40 minutes, the zeta potential value of the copper sulphide suspension became less negative and increased from - 42.9 mV to - 28 mV. Figures 5.5 and 5.6 depict the net interaction plots for a suspension with initial and final zeta potential values of - 42.9 mv and - 28 mv respectively.

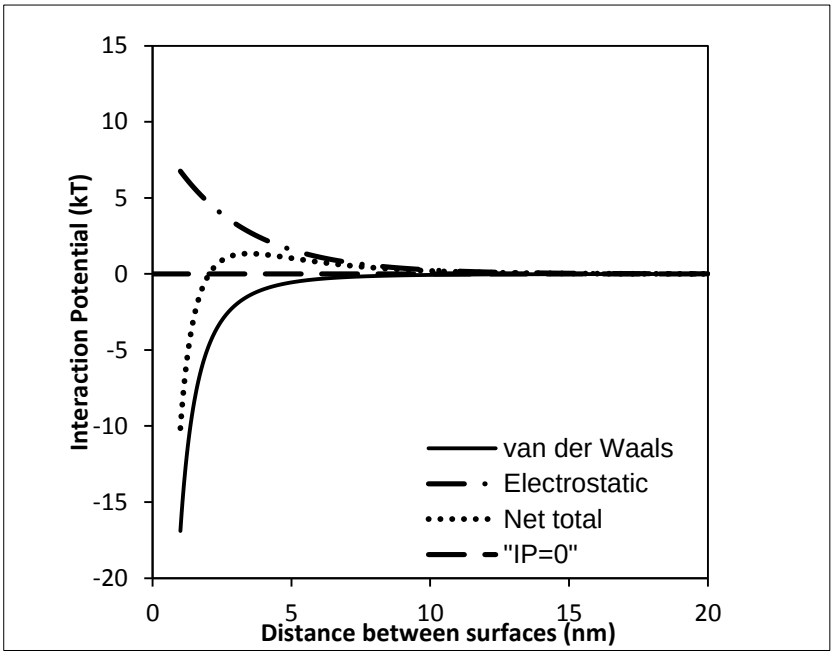

Figure 5.5: Net interaction energy plot for a suspension with a zeta potential of - 42.9 mV

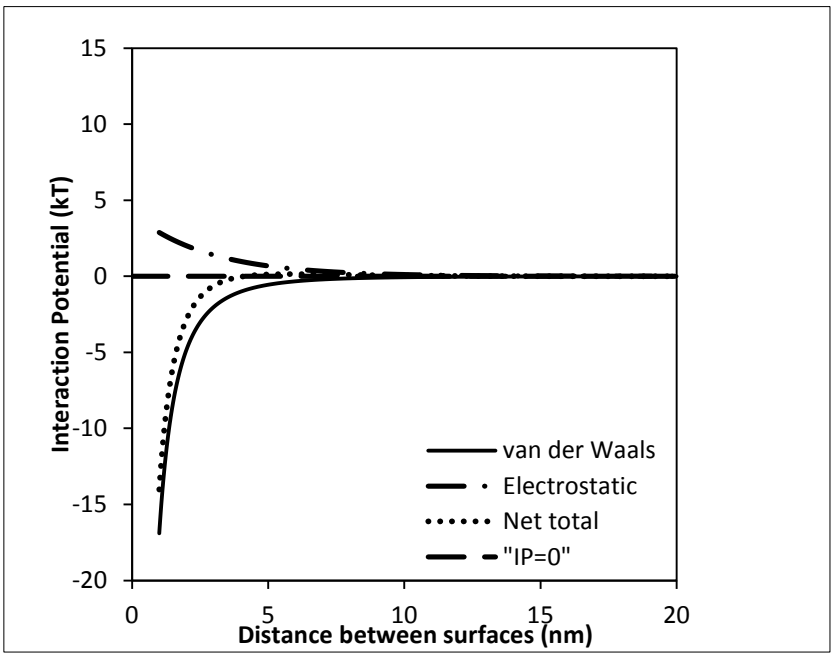

Figure 5.6: Net interaction energy plot for a suspension with a zeta potential of - 28 mV

The net interaction plots on Figures 5.5 and 5.6 show that the suspension shifted from one with repulsive electrostatic forces dominating to one with minimal repulsive forces. The reduction in repulsive forces is due to a reduction in the maximum interaction energy of the suspension. The maximum interaction energy was reduced from 1.34 kT to 0.14 kT for the final and initial suspension zeta potential values respectively. Minimising the repulsive forces enhances the settling rate of the suspension.

At 2 T, an insignificant effect on the zeta potential of a copper sulphide suspension was seen for an exposure time of 10 minutes. However, at this field strength, increasing the exposure time had an observable effect on the zeta potential with a maximum of - 19.5 mV being reached for an exposure time of 40 minutes. The zeta potential of this suspension increased from - 40 mV to - 19.5 mV. The net interaction energy plots for the initial and final zeta potential values of this suspension can be seen on Figures 5.7 and 5.8 respectively.

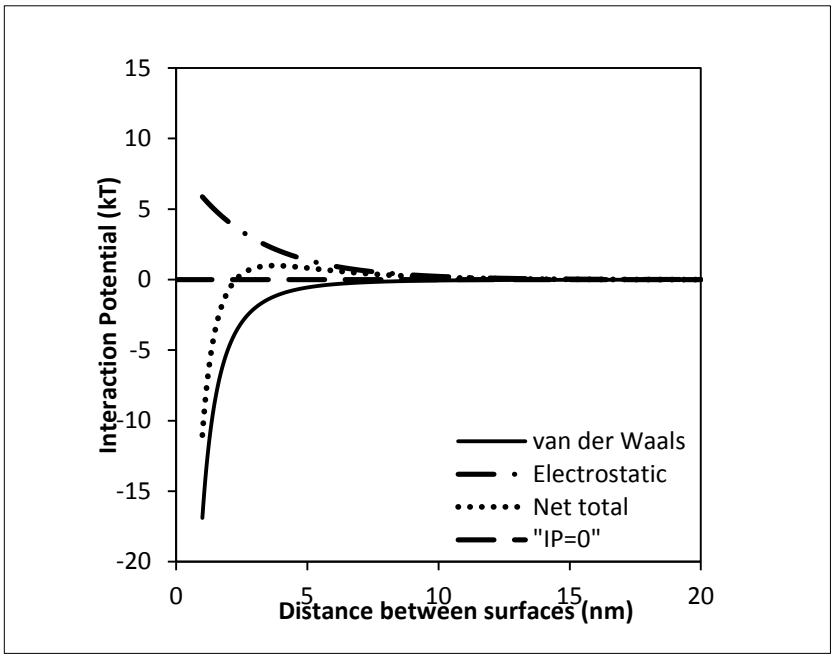

Figure 5.7: Net interaction energy plot for a suspension with a zeta potential of - 40 mV

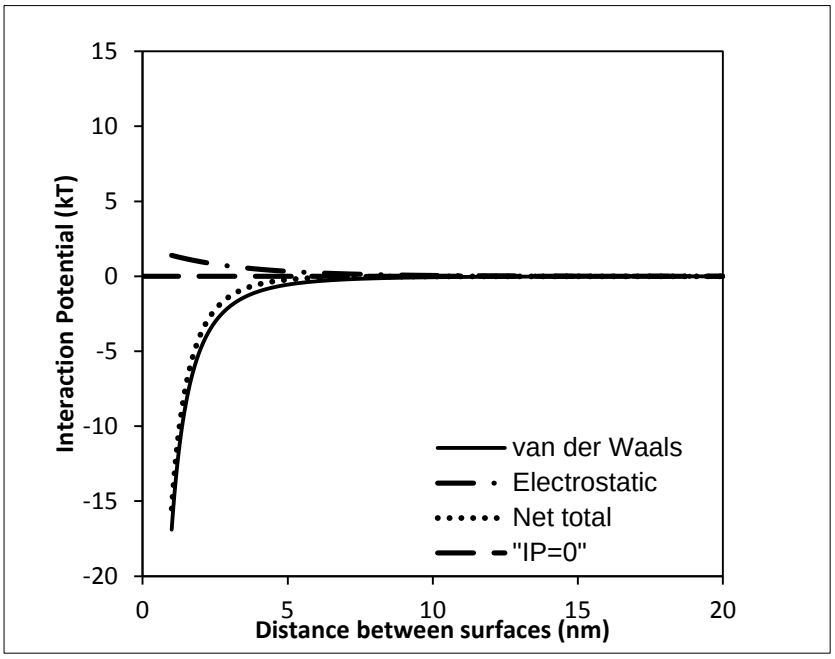

Figure 5.8: Net interaction energy plot for a suspension with a zeta potential of - 19.5 mV

Comparing the plots on Figures 5.7 and 5.8 showed that the maximum interaction energy was reduced from 0.99 kT to - 0.29 kT. A negative value for the maximum interaction energy indicates complete elimination of the repulsive electrostatic forces. Consequently, solely attractive forces are present in the suspension. This favours

aggregation and thus improved settling rates. The final zeta potential of this suspension is therefore within the range for fast settling rates.

5.2.4 Relationship between magnetic field strength and exposure time

From the results obtained, it is evident there exists an inverse relationship between magnetic field strength and exposure time. As the field strength is increased, a shorter exposure time is required to reduce the repulsive electrostatic forces. From equation 3.8, it must be noted that magnetic field strength and exposure time are the only terms that may be varied. The rest of the terms in the equation are constants, for the case where the sample is kept stagnant in the magnetic field. The magnitude of the Lorentz ion shift required to completely eliminate repulsive electrostatic forces for a copper sulphide suspension is constant, that is, there is a minimum value the Lorentz ion shift needs to attain in order to completely eliminate repulsive forces. This value is dependent on these two variables. As a result, there is a trade-off as to which variable is to be maximised in order to achieve this value.

5.2.5 Effect of suspension speed on zeta potential

In the last set of tests (see Table 4.2), copper sulphide particles were oscillated in a homogenous magnetic field. A maximum zeta potential of - 16.5 mV was obtained for an exposure time of 40 minutes at a field strength of 2 T. Zeta potential values of - 22.3 mV and - 20.9 mV were obtained for 1 T and 1.5 T respectively for a 40 minute exposure period.

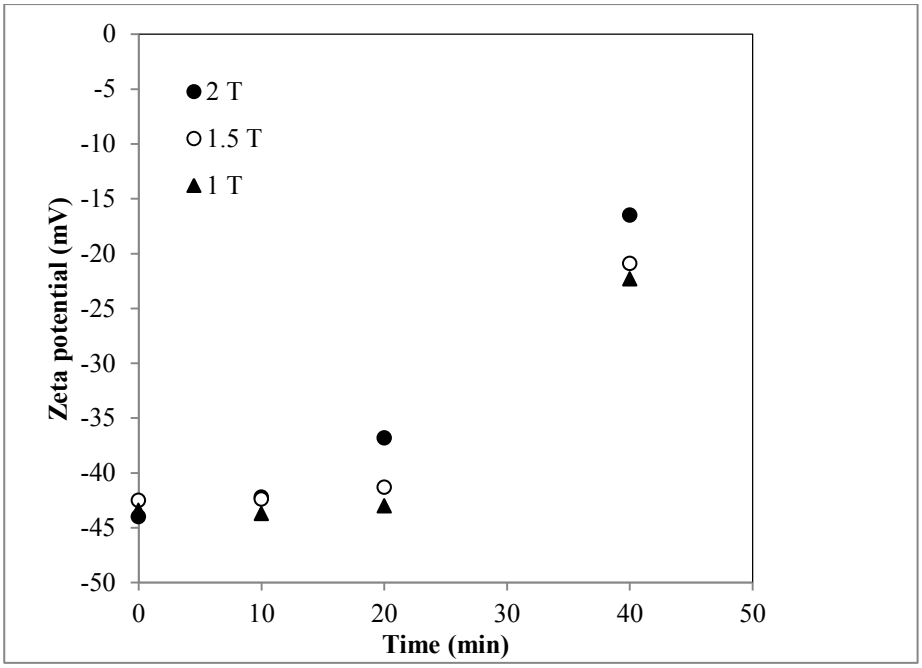

Figure 5.9: Zeta potential of copper sulphide as a function of exposure time at constant field strengths for an oscillating sample

A comparison of the results shown in Figures 5.4 and 5.9 revealed that the zeta potential of copper sulphide particles can be increased, to within the range for fast settling rates, at lower field strengths for the case where the copper sulphide particles are oscillated in the magnetic field. This is because, for the case where the sample holder is oscillated in a homogeneous field, there is a significant reduction in the inter-particle repulsive forces due to an increased Lorentz force. This results from an increase in the suspension speed and thus a greater Lorentz counter-ion ion shift in the Stern layer (Lipus et al, 2001). Comparing Figures 5.4 and 5.9 also showed that an increase in suspension speed reduces the exposure time required for increasing the zeta potential of a suspension to within the range for fast settling rates. For oscillated samples, a larger reduction in the absolute magnitude of the zeta potential was observed at all field strengths after 40 minutes. Furthermore, this result is more pronounced at lower magnetic fields (1 T and 1.5 T). This is because at high field strengths (2T), a significant reduction in the absolute magnitude of the zeta potential of a suspension to within fast settling rates, may be achieved with a non-oscillating sample. Therefore an increase in sample speed does not radically intensify this effect.

Lipus and co-workers (2001) reported that the most successful magnetic water treatment devices are of dynamic type, with an oscillating dispersion through a static magnetic field. It follows that the results obtained by oscillating copper sulphide in a homogeneous field showed improved results.

5.2.6 Control samples

For each experimental run, a control sample was kept. This was done in order to compare zeta potential values between samples that have not been exposed to a magnetic field and those that have. Keeping a control sample ensures that if a change is observed in zeta potential, it is due to the conditions the sample was exposed to and therefore increases the reliability of the results. Figures 5.10, 5.11 and 5.12 depict the change in zeta potential over time for samples that were exposed to a magnetic field and their corresponding control sample.

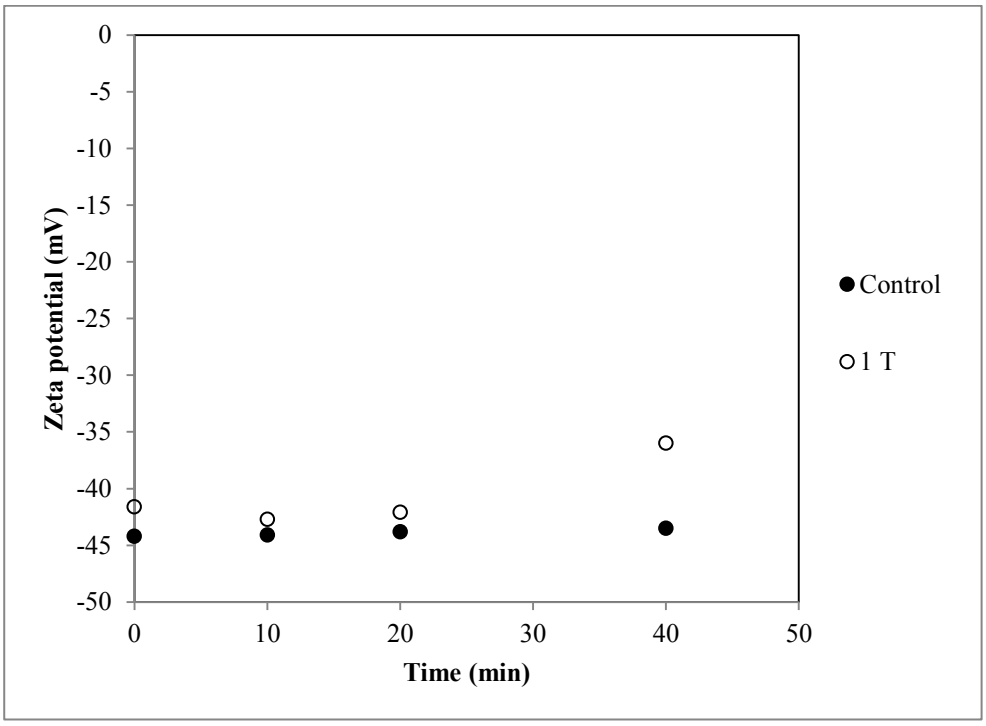

Figure 5.10: Comparison between control and sample exposed to a 1 T magnetic field strength

The plots on Figure 5.10 illustrate that there are no major changes in the zeta potential value of the control sample across all exposure times. This is indicated by the constant

flat slope of the control sample plot. For the 1 T exposure sample no major changes in zeta potential were observed for 10 and 20 minute exposure times. However, an increase in zeta potential is seen for the final exposure time of 40 minutes at 1 T.

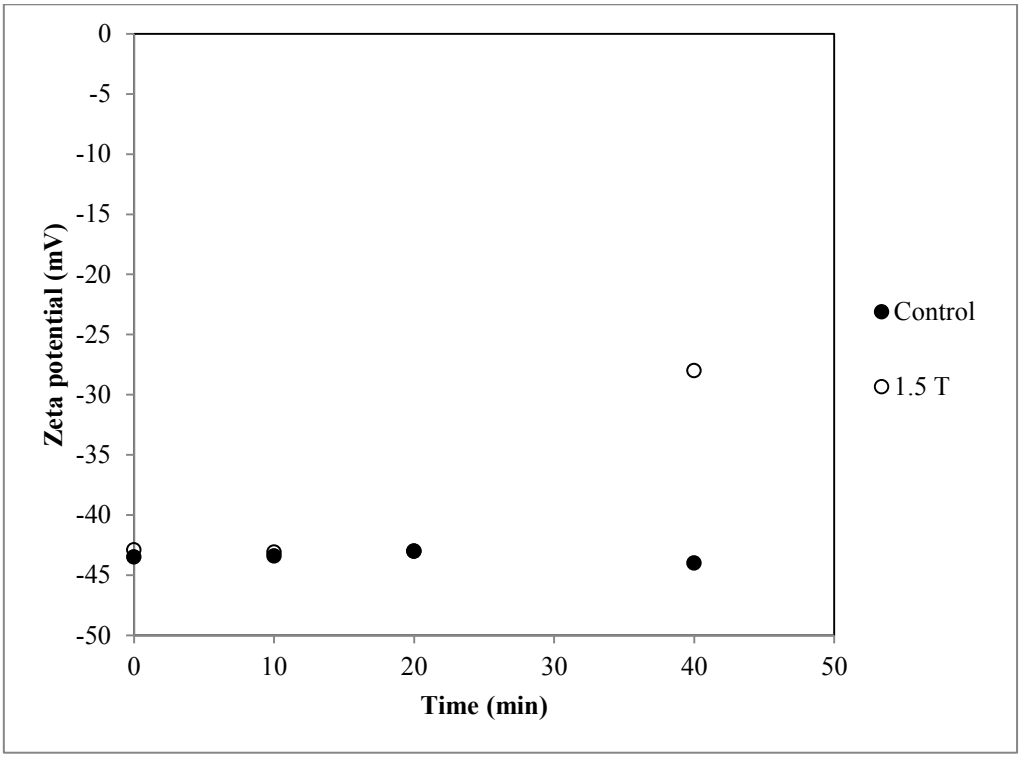

Figure 5.11: Comparison between control and sample exposed to a 1.5 T magnetic field strength

As shown in Figure 5.11, initially the two samples have near identical zeta potential values of - 42.9 mV and - 43.5 mV for the exposure and control samples respectively. At 10 and 20 minutes there in no change in the zeta potential of both samples. It follows that at 1.5 T exposure times of 10 and 20 minutes have no effect on the zeta potential of a copper sulphide suspension. Increasing the exposure time to 40 minutes proved beneficial as the suspension zeta potential increased to - 28 mV. The constant slope of the control sample plot shows that there was no change in the zeta potential of this sample within the magnetic exposure period.

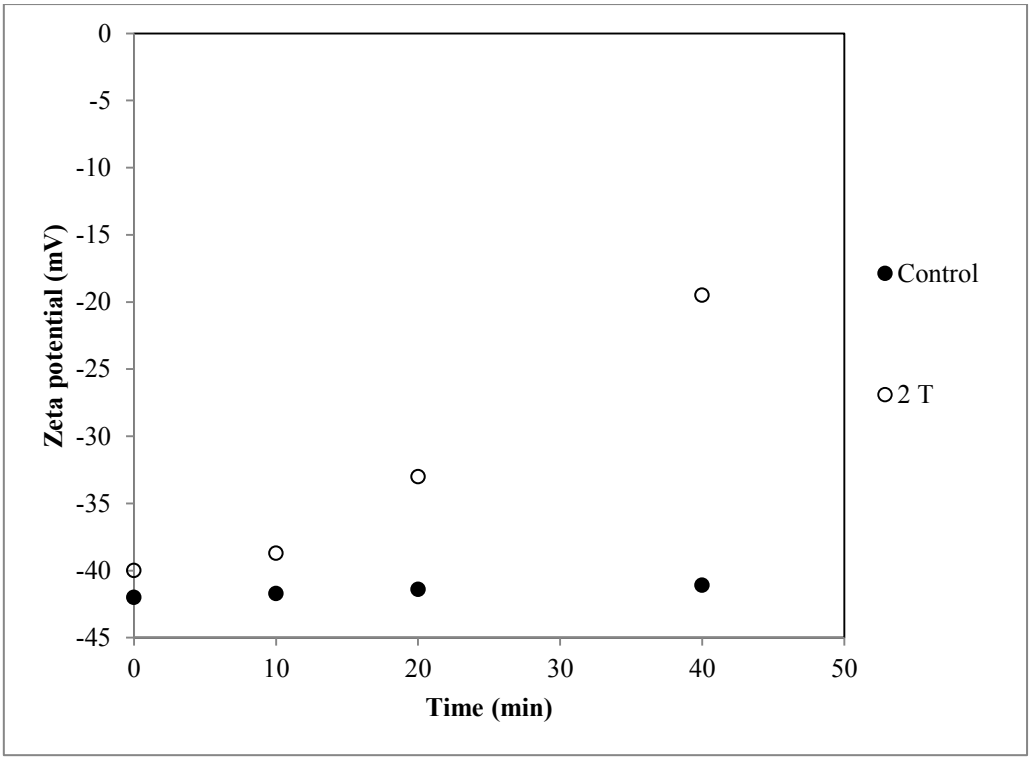

Figure 5.12: Comparison between control and sample exposed to a 2 T magnetic field strength

An increase in the suspension zeta potential is observed with increasing exposure time, for a constant field strength of 2 T. This is depicted in Figure 5.12. In contrast, the control sample remains constant with increasing exposure time.

The time versus zeta potential plots from all the above Figures show that there is no significant change in the zeta potential of all the control samples. One can therefore deduce that changes in suspension zeta potential observed when samples are exposed to a magnetic field are solely due to the Lorentz force exerted on the suspended particles surface by the magnetic field.

5.2.7 Settleability

The settling rate of a copper sulphide suspension may be enhanced by inducing aggregation between the suspended particles. In order to induce aggregation, attractive forces must dominate between particles. Therefore, a reduction in the repulsive electrostatic forces is required. This reduction changes the nature of the electrical double layer surrounding each particle and therefore directly affects the potential at the slipping

plane, also known as zeta potential. Reducing inter-particle repulsive forces, results in a less negative zeta potential and an overall increase in zeta potential. This translates to a decrease in the absolute magnitude of the zeta potential. Vergouw and co-workers (1998) reported that the settling velocity of galena increased when the zeta potential increased (i.e. when the absolute magnitude decreased), while Mokone and co-workers (2010) and Nduna and collaborators (2013) reported that an increase in settleability of copper sulphide particles is associated with a decrease in the absolute magnitude of the zeta potential. On this basis, for the purposes of this study, zeta potential measurements were used as a proxy to indicate settleability.

6. Conclusions & recommendations

6.1 Conclusions

It has been shown that under the specified conditions, the zeta potential of a copper sulphide suspension may be modified by the application of a magnetic field. This is owing to the ion redistribution on the particle surface as a result of the Lorentz force. However, this result is only achievable once a minimum magnetic field strength value of 1 T with a minimum exposure time of 40 minutes has been reached.

The stability of a copper sulphide suspension can be explained using the interplay between attractive and repulsive forces between the suspended particles. This interplay between forces is shown in the results as DLVO plots. From these plots, one may conclude that a reduction in the repulsive electrostatic forces leads to an increase in zeta potential and favours aggregation. Consequently, shorter settling times are expected with the reduction in electrostatic repulsive forces and thus improved settling characteristics.

Magnetic field strength strongly influences the zeta potential of a suspension. Increasing the field strength increases the zeta potential. This effect is amplified in the case where each suspension is oscillated in the magnetic field. Increasing exposure time at a constant magnetic field strength also increases zeta potential. Both variables have a positive relationship with the Lorentz force applied on suspended particles due to magnetic field exposure. In addition to this, as the magnetic field strength is increased, a shorter exposure time is required to increase zeta potential.

This study shows that there is potential in the application of a magnetic field to precipitation processes aimed at treating industrial waste streams with high residual metal ion concentrations, such as acid mine drainage, where the size and charge of the precipitates formed hinder gravitational solid-liquid separation. The technique used in this study not only improves the settling kinetics of a suspension, but does so without the addition of a chemical flocculant and therefore has an added advantage of reducing the volume required for settling. The zero additional chemical additives approach also reduces the environmental impact of industrial waste streams.

6.2 Recommendations

Although the effect of a magnetic field on zeta potential has been shown, it is important to verify how long this effect lasts. It follows that determining the magnetic memory of the system is the first recommendation.

The effect of suspension speed on zeta potential could only be tested at a fixed speed of 2 Hz due to equipment limitations. Testing the effect of a range of speed values on zeta potential would provide a broad spectrum of results. The effect of various speeds on zeta potential should be tested.

Although zeta potential may be used as a proxy to indicate the settleability of a suspension, further settleability tests may be done if there is interest in quantifying the settleability of the suspension.

The recommendations mentioned above can only be achieved with a magnet that possesses the following functions:

1. Multiple sample holder oscillating speed values
2. Increased sample volume for magnetic exposure
3. Higher magnetic field strengths

Unfortunately, the magnetometer used in this study did not support these functions. As a result, these tests could not be done. It is also recommended that the effect of oscillation, on the suspension zeta potential in the absence of a magnetic field, be investigated since the turbulent motion of a conducting fluid may generate spontaneous magnetic fields.

7. References

Attard, P. 2001. Recent advances in the electrical double layer in colloid science. *Current Opinion in Colloid and Interface Science.* 6(4): 366-371

Baker, J.S. & Judd, S.J. 1996. Magnetic amelioration of scale formation. *Water Research.* 30(2): 247-260

Baldyga, J.& Bourne, J. 1984. A fluid mechanical approach to turbulent mixing and chemical reaction. *Chemical Engineering Communications.* 28(4-6): 243-258

Bebie, J., Schoonen, M.A.A., Fuhrmann, M. & Stongin, D. 1998. Surface charge development on transition metal sulphides: An electrokinetic study. *Geochimica et Cosmochimica Acta.* 62(4): 633-642

Bramley, A.S., Hounslow, M.J. & Ryalls, R.L. 1997. Aggregation during precipitation from solution. Kinetics for calcium oxalate monohydrate. *Chemical Engineering Science.* 52(5): 747-756

Capretto, L., Cheng, W., Hill, M. & Xunli, Z. 2011. Micromixing within microfluidic devices. *Top Curr Chem.* 304: 27-68

Chan, D. 1976. Electrical Double Layer Interactions under Regulation by Surface Ionization Equilibria--Dissimilar Amphoteric Surfaces. *Royal Society of Chemistry.* 72(1): 2844-2865

Chan, D., Healy, T.W., Supasiti, T. & Usui, S. 2006. Electrical double layer interactions between dissimilar oxide surfaces with charge regulation and Stern–Grahame layers. *Journal of Colloid and Interface Science.* 296(1): 150-158

Chiang, Y.L., Nathoo, J. & Lewis, A.E. 2007. Investigating the control of manganese sulphide precipitation. *Journal of The Southern African Institute of Mining and Metallurgy.* 107(4): 231-236

Derjaguin, B.V., Churaev, N.V. & Muller, V.M. 1987. Surface Forces. New York: Consultants Bureau.

Feng, D., Aldrich, C. & Tan, H. 2000. Treatment of acid mine water by use of heavy metal precipitation and ion exchange. *Minerals Engineering.* 13(6): 623-642

Fullston, D., Fornasiero, D. & Ralston, J. 1999. Zeta potential study of the oxidation of copper sulfide minerals. *Colloids and Surface A: Physicochemical and Engineering Aspects.* 146(1-3): 113-121

Green, D. 2002. Crystallizer mixing: Understanding and modeling crystallizer mixing and suspension flow. In: A.S. Myerson, ed. Handbook of crystallization. Woburn: Butterworth-Heinmann. 180-198

Hartel, R.W., Gottung, B.E., Randolph, A.D. & Drach, G.W. 1986. Mechanisms and kinetic modeling of calcium oxalate crystal aggregation in a urinelike liquor. Part I. *American Institute of Chemical Engineers.* 32(7): 1176-1185

Higashitani, K., Iseri, H., Okuhara, K., Kage, A. & Hatade, S. 1994. Magnetic effects on zeta potential and diffusivity of nonmagnetic colloidal particles. *Journal of Colloid and Interface Science.*172(2): 383-388

Hounslow, M.J., Ryall, R.J. & Marshall, V.R. 1988. A discretized population balance for nucleation, growth and aggregation. *American Institute of Chemical Engineers.* 34(11): 1821-1832

Jackson, E. 1986. Hydrometallurgical Extraction and Reclamation. West Sussex, England: Ellis Horwood Limited.

Karpinski, P.H. & Wey, J.S. 2002. Precipitation processes. In: A.S. Myerson, ed. Handbook of crystallization. Woburn: Butterworth-Heinmann. 141-159

Kirwan, D.J. & Orella, C.J. 2002. Crystallization in the pharmaceutical and bioprocessing industries. In: A.S. Myerson, ed. Handbook of crystallization. Woburn: Butterworth-Heinmann. 247-264

Knight, R.D. Physics for scientists and engineers: A strategic approach. San Francisco, United States of America: Pearson Addison-Wesley

Kozic, V. & Lipus, L.C. 2003. Magnetic water treatment for a less tenacious scale. *Journal of Chemical Information and Computer Science.* 43(6): 1815-1819

Lewis, A. & van Hille, R. 2006. An exploration into the sulphide precipitation method and its effect on metal sulphide removal. *Hydrometallurgy.* 81(2-3): 197-204

Lewis, A.E. 2010. Review of metal sulphide precipitation. *Hydrometallurgy.* 104(2): 222-234

Lipus, L.C., Krope, J. & Crepinsek, L. 2001. Dispersion Destabilization in Magnetic Water Treatment. *Journal of Colloid and Interface Science.* 236(1): 60-66

Mokone, T.P., van Hille, R.P. & Lewis, A.E. 2010. Effect of solution chemistry on particle characteristics during metal sulfide precipitation. *Journal of Colloid and Interface Science*. 351(1): 10-18

Mokone, T.P., Lewis, A.E. & van Hille, R.P. 2012. Effect of post precipitation on surface properties of colloid metal sulphide precipitates. *Hydrometallurgy.* 119-120: 55-66

Mullin, J.W. 2001. Cystallization. 4th ed. Woburn: Butterworth-Heinmann.

Myerson, A.S. & Ginde, R. 2002. Crystals, crystal growth, and nucleation. In: A.S. Myerson, ed. Handbook of crystallization. Woburn: Butterworth-Heinmann. 35-67

Myerson, A.S. & Schwartz, A.M. 2002. Solutions and solution properties. In: A.S. Myerson, ed. Handbook of crystallization. Woburn: Butterworth-Heinmann. 4-34

Nduna, M.K. 2013. Post precipitation treatment of copper sulphide particles to improve settleability. Thesis. Department of Chemical Engineering. University of Cape Town

Nduna, M., Rodriguez-Pascual, M. & Lewis, A.E. 2013. Effect of dissolved precipitating ions on the settling characteristics of copper sulphide. *Journal of The Southern African Institute of Mining and Metallurgy.* 113(5): 435-439

Ohshima, H. 1995. Effective Surface potential and Double-Layer Interaction of Colloidal Particles. *Journal of Colloid and Interface Science.* 174(1): 45-52

Ottewill, R.H. 1977. Stability and instability in disperse systems. *Journal of Colloid and Interface Science.* 58(2): 357-373

Overbeek, J.TH.G. 1977. Recent developments in the understanding of colloidal stability. *Journal of Colloid and Interface Science.* 58(2): 408-422

Overbeek, J.TH.G. 1982. Strong and weak points in the interpretation of colloidal stability. *Advances in Colloid and Interface Science.* 16(1): 17-30

Overbeek, J.TH.G. 1984. Interparticle forces in colloid science. *Powder Technology.* 37(1): 195-208

Parker, M.R., van Kleef, R.P.A.R., Myron, H.W. & Wyder, P. 1982. Study of particle behaviour in high field magnetic flocculation. *IEEE Transactions on Magnetics.* MAG-18(6): 1647-1649

Parsons, S.A., Judd, S.J., Stephenson, T., Udol, S. & Wang, B-L. 1997. Magnetically augmented water treatment. *Institution of Chemical Engineers.* 75(2): 98-104

Silberberg, M.S. 2006. Chemistry: The molecular nature of matter and change. New York, United States of America: McGraw-Hill

Shiebl, B., Babick, F. & Stintz, M. 2012. Calculation of double layer interaction between aggregates. *Advanced Powder Technology*. 23(2): 139-147

Shneider, C., Hanisch, M., Wedel, B., Jusifi, A. & Ballauf, M. 2011. Experimental study of electrostatically stabilized colloidal particles: Colloidal stability and charge reversal. *Journal of Colloid and Interface Science.*358(1): 62-67

Svoboda, J. 1982. Magnetic flocculation and treatment of fine weakly magnetic minerals. *IEEE Transactions on Magnetics.* MAG-18(2): 796-801

Ulrich, J. & Stelzer, T. 2011. In: Kirk Othmer Encyclopaedia in Chemical Technology. England: John Wiley and Sons Ltd.

van Kleef, R.P.A.R., Parker, M.R., Myron, H.W. & Wyder, P. 1982. Sedimentation of colloids in high magnetic fields. *IEEE Transactions on Magnetics.* MAG-18(6): 1650-1652

Veeken, A.H.M., de Vries, S., van der Mark, A. & Rulkens, W.H. 2003. Selective precipitation of heavy metals as controlled by a sulphide-selective electrode. *Separation science and Technology.* 38(1): 1-19

Velev, O.D. & Bhatt, K.H. 2006. On chip manipulation and assembly of colloidal particles by electric fields. *The Royal Society of Chemistry.* 100(2)*:*738-750

Vergouw, J.M., Difeo, A., Xu, Z. & Finch, J.A. 1998. An agglomeration study of sulphide minerals using zeta potential and settling rate. Part I: Pyrite and galena. *Minerals Engineering.* 11(2): 159-169

Wang, Y., Pugh, R.J. & Fossberg, E. 1994. The influence of interparticle surface forces on the coagulation of weakly magnetic mineral ultrafines in a magnetic field. *Colloids and surfaces.* 90(2-3): 117-133

Weigl, B.H., Bardell, R.L. & Cabrera, C.R. 2003. Lab on a chip for drug development. *Advanced Drug Delivery Reviews.* 55(3): 349-377

Zaidi, N.S., Sohalili, J., Muda, K. & Silanpaa, M. 2013. Magnetic field application and its potential in water and wastewater treatment systems. *Separation and Purification Reviews.* 43(3): 206-240

8. Appendices

Appendix A

Flow characterisation in T-mixer

$$Re = \frac{uD_H\rho}{\mu}$$

Where u is the fluid velocity ($m.s^{-1}$), D_H is the hydraulic diameter (m), ρ is the fluid density ($kg.m^{-3}$) and μ is the fluid dynamic viscosity ($kg.m^{-1}.s^{-1}$).

For a round pipe mixing channel, the hydraulic diameter is equal to the inner pipe diameter.

$D_H = 0.004$ m

$\rho = 998.29$ $kg.m^{-3}$ (density of water at ambient conditions)

$\mu = 0.001$ (dynamic viscosity of water at ambient conditions)

For $Re \leq 2000$ the flow may be characterised as laminar

For $2000 < Re < 3000$ the flow may be characterised as transient

For $Re \geq 3000$ the flow may be characterised as turbulent

$$u = \frac{Q}{A}$$

Where Q is the volumetric flowrate ($m^3.s^{-1}$) and A is the mixing channel area (m^2).

Table 8.1: Flow characterisation for various pump speeds in mixing channel

Pump speed (rpm)	t (s)	V (mL)	Q (m^3/s)	u (m/s)	Re (-)	Flow
566	30	172	5.7E-06	0.46	1816.41	laminar
691	30	205	6.8E-06	0.54	2164.90	transient
834	30	240	8.0E-06	0.64	2534.52	transient
1178	30	321	1.1E-05	0.85	3389.92	transient
1298	30	360	1.2E-05	0.95	3801.78	transient
1427	30	410	1.4E-05	1.09	4329.81	turbulent
1777	30	480	1.6E-05	1.27	5069.04	turbulent
1904	30	540	1.8E-05	1.43	5702.67	turbulent

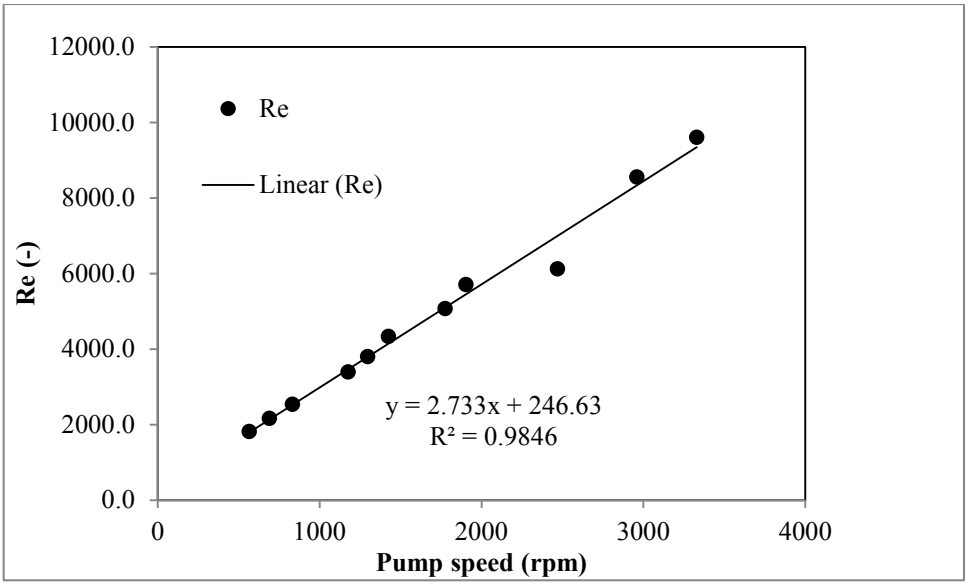

Figure 8.1: Calibration plot for pump speed and Re

Appendix B

Plots showing the change in zeta potential for control samples used in dynamic tests

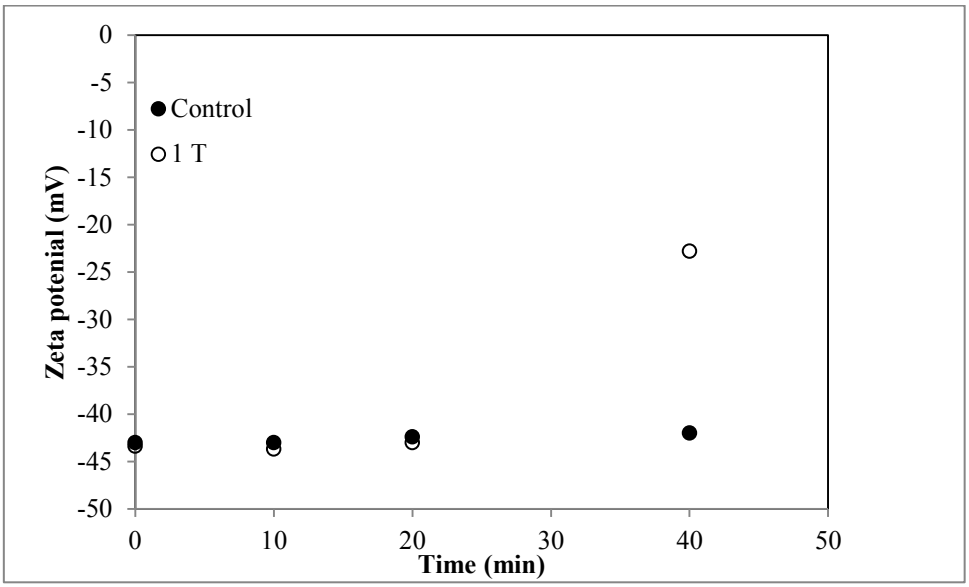

Figure 8.2: Comparison between control and exposure samples at 1 T

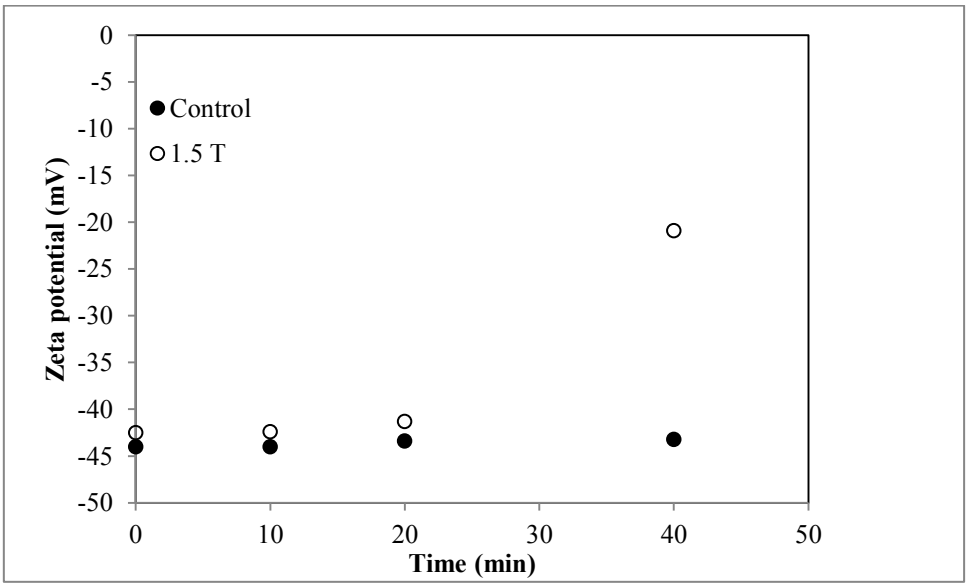

Figure 8.3: Comparison between control and exposure samples at 1.5 T

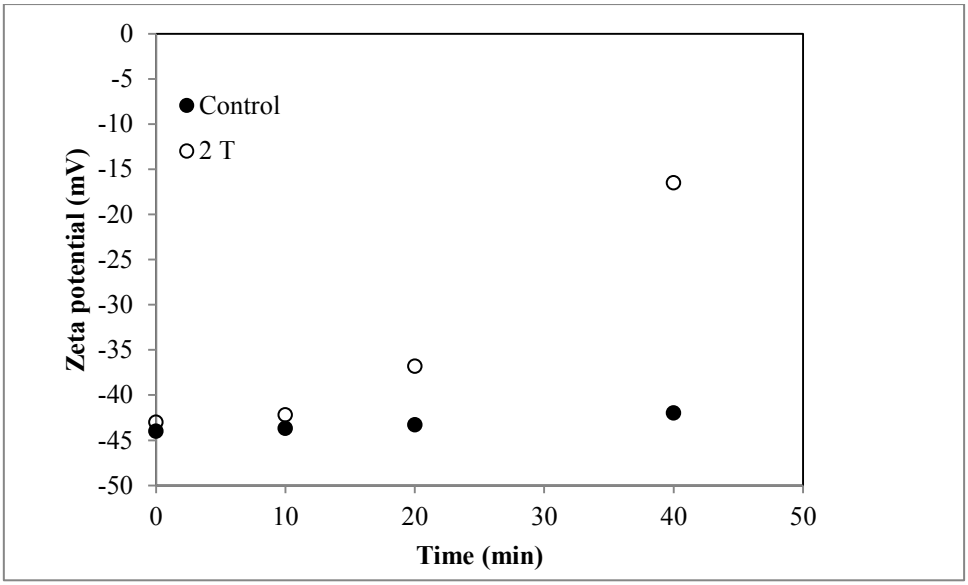

Figure 8.4: Comparison between control and exposure samples at 2 T

Appendix C

Images showing suspended particles and settled particles in sample cuvette pre and post magnetic exposure respectively:

Figure 8.5: suspended particles pre magnetic exposure

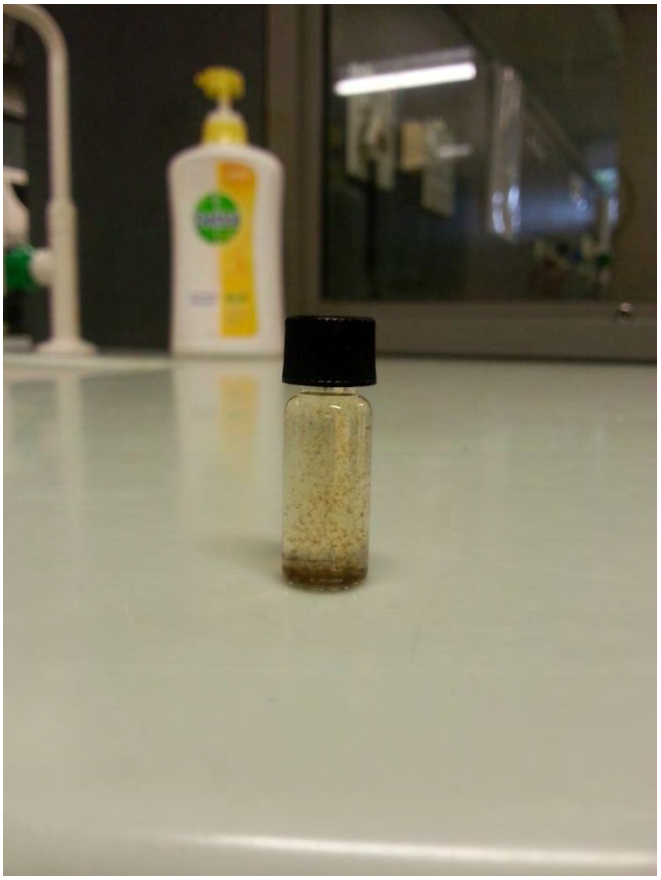

Figure 8.6: settled particles post magnetic exposure